Analytical Biochemistry 630 (2021) 114323

Contents lists available at ScienceDirect

Analytical Biochemistry

journal homepage: www.elsevier.com/locate/yabio

Recent advances in FRET-Based biosensors for biomedical applications

Mahsa Imani [a], Nasrin Mohajeri [a,**], Mojgan Rastegar [b,c], Nosratollah Zarghami [a,d,e,*]

[a] Department of Medical Biotechnology, Faculty of Advanced Medical Sciences, Tabriz University of Medical Sciences, Tabriz, Iran
[b] Department of Biochemistry and Medical Genetics, Max Rady College of Medicine, Rady Faculty of Health Sciences, University of Manitoba, Winnipeg, Canada
[c] Regenerative Medicine Program, Max Rady College of Medicine, Rady Faculty of Health Sciences, University of Manitoba, Winnipeg, Canada
[d] Department of Medicine, Faculty of Medicine, Istanbul Aydın University, Istanbul, Turkey
[e] Department of Clinical Biochemistry and Laboratory Medicine, Faculty of Medicine, Tabriz University of Medical Sciences, Tabriz, Iran

ARTICLE INFO

Keywords:
Biomedical application
Biosensor
Cancer biomarker
Cellular imaging
FRET
Ratiometric imaging

ABSTRACT

Fluorescence resonance energy transfer (FRET)-based biosensors are effective analytical tools extensively used in fields of biomedicine, pharmacology, toxicology, and food sciences. Ratiometric imaging of substantial cellular processes, molecular components, and biological interactions is widely performed by these biosensors. A variety of FRET-based biosensors have provided comprehensive insights into underlying mechanisms of pathological conditions in live cells, tissues, and organisms. Moreover, integration of FRET-based biosensors with the current bioanalytical techniques allows for accurate, rapid, and sensitive diagnosis and proposes the advanced strategies for treatment. Precise analysis of ligand-receptor interactions by FRET-based biosensors has presented a basis for determination of novel therapeutic agents. Therefore, this study was designed to review the recent developments in FRET-based biosensors and their biomedical applications. In addition, characteristics, challenges, and outlooks of these biosensors were discussed.

1. Introduction

Employment of fluorescence-based technologies in bioanalytical assays has introduced novel quantitative tools for elucidating biomedical processes [1]. Non-radiative resonance energy transfer (RET) approaches have been developed to take advantages from fluorescence (FRET), bioluminescence (BRET), or chemiluminescence (CRET) molecules [2,3]. FRET has received a great deal of interest in various fields including biological and biomedical research [4–6]. High sensitivity, specificity, distance dependency, fast response, simplicity, and being a homogeneous assay are the main properties of FRET [7–9]. Also, spatiotemporal distribution of fluorescent materials along with real-time signals is considered among FRET advantages [9–11]. FRET-based biosensors have served a great potential in determination of cellular dynamics [12] and molecular interactions [13], detection of conformational changes in proteins (e.g., amyloid-β) [14] and nucleic acids (e.g., nucleosomes) [15], quantification of intracellular ions (e.g., Ca^{2+}) [16], and accurate identification of cancer biomarkers [5],such as micro RNAs (miRNAs) [17,18]. In addition, *in-vitro* monitoring of signaling pathways and associated small molecules (e.g., protein kinases) [19], non-invasive imaging of cellular components [20], cell cycles, proliferation, and apoptosis have been profitably performed by FRET-based biosensors [21]. However, several unmet challenges including low stability, intracellular aggregation, and signal overlap have restricted application of these biosensors for multiplexed imaging at cellular and subcellular scales [22]. Ratiometric FRET probes have introduced an effective platform for multiplexed imaging of two or more targets simultaneously in a single sample [23]. Conjugation of FRET-based biosensors with nanoparticles (NPs) could enhance photophysical properties of these biosensors [24]. Besides, labeling FRET-based biosensors with nanocarriers and cell-specific markers could preserve biosensor integrity during membrane internalization and enable the targeted delivery of biosensors, respectively [23,25]. For *in vivo* and tissue-depth imaging, FRET-based biosensors could be transmitted to specific cells or tissues either through electroporation, viral delivery, or injection with the transfected cell lines, or could be genetically expressed in an engineered transgenic cell line and organism [21,26–28]. Integration of FRET-based biosensors with conventional immunoassays,such as inspired enzyme-linked immunosorbent assay (ELISA) has significantly enhanced sensitivity and specificity of target detection [29]. Direct visualization of ligand-receptor interactions by FRET-based immunosensors has provided novel strategies for point-of-care (POC) detection and therapeutic approaches [30,31]. Accordingly, in this

* Corresponding author. Department of Clinical Biochemistry and Laboratory Medicine, Faculty of Medicine, Tabriz University of Medical Sciences, Tabriz, Iran.
** Corresponding author. Department of Medical Biotechnology, Faculty of Advanced Medical Sciences, Tabriz University of Medical Sciences, Tabriz, Iran.
E-mail addresses: Mohajerin@tbzmed.ac.ir (N. Mohajeri), Zarghamin@gmail.com (N. Zarghami).

https://doi.org/10.1016/j.ab.2021.114323
Received 10 June 2021; Received in revised form 21 July 2021; Accepted 29 July 2021
Available online 31 July 2021
0003-2697/

review study, it is attempted to describe FRET principle and its prominent role in designing biosensors. Biomedical application of FRET-based biosensors is explained and the main characteristics and challenges of these biosensors are discussed.

1.1. Principle of FRET

FRET is a photophysical phenomenon whereby resonance energy of a donor fluorophore is non-radiatively transferred to an acceptor through dipole-dipole interactions [7]. Quantification of energy transfer is primarily influenced by several factors including donor and acceptor (FRET pair) proximity, donors' quantum yield (QY), absorption coefficient (ε_{max}) of acceptor, parallel orientation of FRET pair dipoles, and substantial overlap between donor emission spectra and acceptor excitation or absorption spectra (Fig. 1a). Physical dipole-dipole interaction of an excited donor stimulates acceptor to the excited state along with donor relaxation to non-fluorescent ground state ($D^* + A \rightarrow D + A^*$) (Fig. 1b) [32]. The main distance between FRET pair (r) ranges from 1 to 10 nm to obtain the desired efficiency [33]. Rate of distance-dependent energy is scaled with Förster distance R0, where FRET efficiency is equal to 0.5 (50%) [34]. Förster distance is determined by the following equation:

$$R_0 = 0.21\left[k^2 Q_D n^{-4} J(\lambda)\right]^{\frac{1}{6}}$$

where, k is orientation factor of donor and acceptor dipoles, QD is donors' QY, n is a medium-related refractive index, and $J(\lambda)$ is related to spectral overlap between donor emission and acceptor absorption. Thereby, FRET efficiency is computed as:

$$E = \frac{R_O^6}{R_O^6 + r^6}$$

As a matter of fact, FRET is a nanoscale ruler in terms of distance-related efficiency, enabling spatiotemporal analysis of biomolecules, such as multi-subunit proteins, determination of protein folding, and monitoring density of biological membranes [35,36]. A great number of well-established fluorescent substrates and quenching molecules are employed as FRET pairs, categorized into three main groups: organic dyes, fluorescent proteins (FPs), and NPs. Organic dyes,such as FAM,

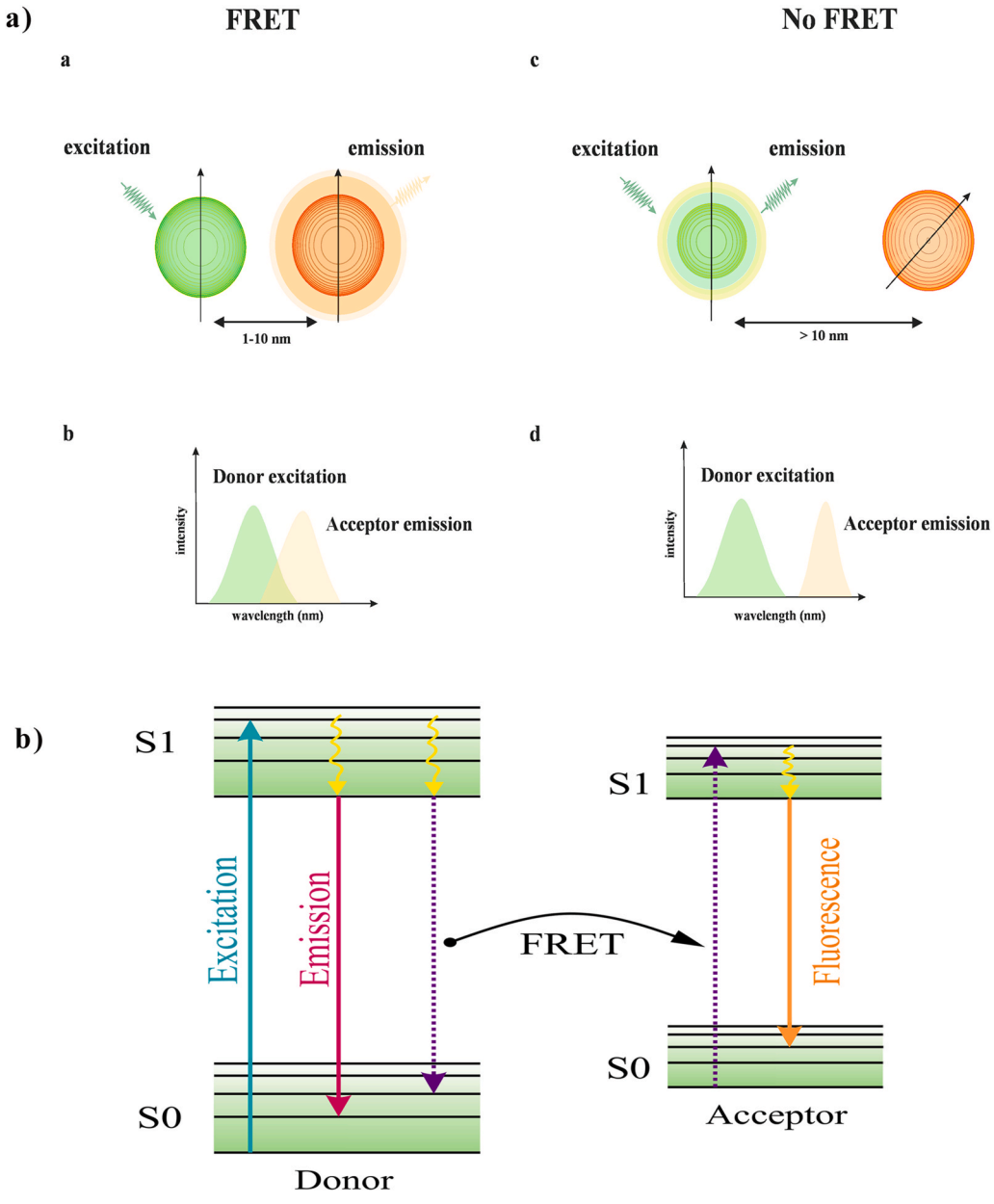

Fig. 1. Principle of FRET. **a)** The main criteria influencing occurrence of FRET: a, b Donor and acceptor distance (r) must be less than or comparable to R0 at which 50% FRET occurs, as well as establishment of parallel orientation of dipole-dipole interaction, and spectral overlap between donor emission and acceptor excitation. No FRET occurs when c, d r is longer than 10 nm (r ≫ R0), orientation of dipoles of donor and acceptor is perpendicular, and donor emission spectrum is separated from acceptor excitation spectrum. **b)** Jablonski diagram of FRET. A donor chromophore (D) at ground state (S0) absorbs light and is excited to an electronically higher state (S1*). D* then emits part of its energy as fluorescence during relaxation to the S0. In the presence of a suitable acceptor (A), energy of D* is transferred to the A through dipole-dipole interaction leading to excitation of the A to S1*.

Cyanine, and Texas Red are reactive fluorophores that bind to proteins and nanocarriers for bioimaging and diagnostic purposes [37–39]. Generally, optical properties of organic dyes are solvent-dependent. Wide-range absorption (λ_{abs}, max 310–750 nm) and emission (λ_{emi}, max 380–700 nm), high photoluminescence QY (Φ_{QY} 0.2–1), absorption coefficient ($\log_{10}(\varepsilon_{max}) < 2.5$ $cm^{-1}M^{-1}$), emission line width ($\sigma_{emi} >$ 7000 cm^{-1}), and large stoke shift ($\Delta\lambda = 186$ nm or $\Delta\nu = 8572$ cm^{-1}) along with solubility, small size (maximum 150 atoms), and simplicity of bioconjugation are the main properties of these dyes [40–43]. Nevertheless, high photobleaching rate at near-infrared, poor aqueous stability, and cytotoxicity could limit intracellular applications of fluorescent dyes in some cases [44–46]. FPs, such as green FPs (GFP) (e.g., mClover3), red FPs (RFP) (e.g., mCherry), yellow FPs (YFP) (e.g., cp173Venus), and cyan FPs (CFP) (e.g., mTurquoise2) are genetically encoded and widely used as FRET pairs [47,48]. Photostability, pH stability (pK_a 2.5–6.5), and photoconversion are critical properties of FPs for optical assays. FPs are ~25-kD (4.2 nm in length and 2.4 nm in diameter) oligomers with the controlled N- or C-terminal [49]. Optical properties of FPs including λ_{abs} max (380–600 nm), λ_{emi} max (440–650 nm), Φ_{QY} (0.1–~1), wide-range photobleaching half-times (2.7–530 s), ε_{max} (10^4–10^5 $cm^{-1}M^{-1}$), rely on rigidity of protein structure, chemical environment, and excitation power in a linear manner [41,49,50]. However, long-term maturation, non-specific self-assembly, and irreversible complementation could restrict application of some FPs [51]. Fluorescent NPs, such as gold NPs (AuNPs), graphene quantum dots (GQDs), graphene oxide (GO), semiconductor quantum dots (QDs), and upconversion NPs (UNPC) are extensively used in designing FRET-based biosensors [26,52,53]. AuNPs and paramagnetic NPs have been reported to increase emission intensity and provide a solid support for effective immobilization of FRET probes in hybridization-based biosensors, respectively [54,55]. Controllable size and shape, higher emission intensity (551 nm), ε_{max} (10^8–10^{10} $cm^{-1}M^{-1}$), the enhanced photostability, and significant photobleaching resistivity are the main characteristics of fluorescent NPs [56–58]. Currently used FRET pairs in designing biosensors are mentioned in Tables 1–4. FRET-based biosensors are mainly established based on several principles including typical single FRET probe [59], dual-mode FRET [60], 3D multiplexing [61], hybridization probes [62], sandwich co-hybridization [63], and enzymatic digestion [64]. Regarding design principle and diversity of FRET pairs, a large number of biosensors have been developed for various biomedical purposes [65].

2. FRET-based biosensors for cellular and molecular detection

FRET-based biosensors are widely used to provide comprehensive information about biological processes,such as cell cycling, metabolism, and signaling pathways [29,66,67]. Quantitative analysis of molecular components including cholesterol derivatives, hemoglobin, cell-specific antigens, and miRNAs has been carried out by FRET-based biosensors [5,68,69].

2.1. Detection of cancer biomarker

Accurate identification of cancer-related biomarkers is of great importance for early diagnosis of cancer. The miRNAs are non-coding RNA molecules known to be involved in initiation and progression of carcinogenesis as well as regulation of apoptosis [70]. Identification of cancer-related miRNAs could provide substantial information on early detection of cancer and designing efficient treatment strategies [18,71]. In this regard, a great number of FRET-based biosensors have been successfully designed (Table 1).

Wang et al., detected miR-21–5p and miR-92a-3p in HeLa cell exosomes using a FRET-based biosensor. This biosensor acted based on target-assisted signal amplification (Fig. 2a). The stem-loop structure of Cysteine5 (Cy5) -labeled probes opened exclusively upon miR-21 hybridization, exposing binding site for AuNP-labeled primers. Proximity of Cy5-labeled probe and AuNP-labeled primers after hybridization resulted in FRET by quenching Cy5 fluorescence signal. Strand displacement of primers through enzymatic induction led to release of miR-21 from oligonucleotide duplex. Recycling of miRNA by strand displacement considerably amplified fluorescence signal. This biosensor represented high potential for miR-21 detection in a linear manner with limit of detection (LOD) of 1.5 fM [79]. Accordingly, FRET-based biosensing assays have ensured sensitive detection of miRNAs *in -situ* compared to prevalent techniques, such as northern blots, microarray analysis, and reverse transcription-polymerase chain reaction [79,80]. FRET-based biosensors have been utilized for accurate detection of cancer biomarkers,such as sarcosine and aurora kinase A (AURKA) in prostate and epithelial cancers, respectively [55,81]. AURKA is a multifunctional serine-threonine kinase associated with cell cycle progression and its overexpression is a major hallmark of epithelial cancers. In this regard, in a study, a highly specific FRET-based biosensor was established for identification of conformational changes and spatiotemporal activation of AURKA induced by autophosphorylation of Threonine (Thr) 288 residue. The biosensor comprised of AURKA complete sequence labeled with the engineered GFP and mCherry. The biosensor functionally replaced endogenous AURKA in U2OS human osteosarcoma cells to identify kinase activation throughout cell cycle. Following autophosphorylation of Thr 288, conformational changes in AURKA resulted in proximity of donor and acceptor and occurrence of FRET [81]. Likewise, in a research, enzymatic activity of prostate-specific antigen (PSA) was

Table 1
Recently developed FRET-based biosensors for detection of cancer-related miRNAs.

Principle of FRET biosensor	Target miRNA	Donor/acceptor	Linear range of detection	LOD	miRNA source	Ref.
Target-probe hybridization	miRNA-21, miRNA-122, and miRNA-223	TOTO-1/Cy3, Cy3.5, Cy5	0.02–10 nM	0.5 nM	Human serum samples	[72]
	mRNA-21, mRNA-155 and Let-7a	AgNCs/CdTe quantum dot	5.0 pM–50 nM	1.2 pM	human blood plasma	[73]
	miRNA-150	FAM/BHQ1	100 fM–10 nM	38 fM	human blood	[74]
	hsa-miR-146b-5p	FAM/TAMRA	10 pM–100 nM	6 pM	Human colon, breast, and thyroid cancer cells, fibrosarcoma, and normal colonic epithelial cell lines Blood sample, HeLa cells,	[75]
	miR-20a miR-21	Terbium/ Cyanine5.5	30–300 pM	1.7 pM	Human blood, cells and tissues	[18]
	miR-21	FAM/Graphene oxide	1–8 nM	1 nM	Human serum samples	[76]
Sandwich co-hybridization	miRNA-195	CaF2:Yb, Ho@SiO_2/Au NPs	2–500 nM	–	Clinical samples (Plasma, tissues, cells)	[77]
	miRNA-155	La(III)-MOF/Ag NPs	2.70–0.01 pM	5.20 fM	Human serum samples	[63]
Catalytic hairpin assembly	miR-21 and miR-20a	Terbium/ Cyanine5.5	0–400 pM	1.8 pM	Human tissues	[78]

Table 2
Recently developed FRET-based biosensors for *in vitro* imaging.

Principle	Emission region	Imaging target	Donor/Acceptor	LOD	Properties	Ref.
Ratiometric imaging	NIR	Biothiols (cysteine, homocysteine, and glutathione)	BODIPY/rhodamin	0.26 μM	High sensitive Excellent linear relationship	[20]
	UV	Mitochondrial SO_2 derivatives (hso3-/so32-)	Phenothiazine oxide/e)-4-(4-(dimethylamino)styryl)-1-alkylpyridin-1-ium	11.03 μM	Rapid monitoring and quantitative detection	[92]
		Mitochondrial cysteine	Coumarin/Nethyl-2-styrylquinolinum	26.3 nM	Highly sensitive and convenient monitoring of Cys metabolic process, good cell permeability	[93]
single chain probe based imaging	NIR	Rho GTPases	miRfp670–miRfp720	–	Minimal cross-excitation, simultaneous imaging, optimal compatibility, and deep tissue penetration. Monitoring cell dynamics and metabolic functions at cell and tissue levels	[89]
	UV	Membrane-tethered type Matrix metalloproteinases	FAM/dabcyl	–	Effective tumor imaging, High specificity and binding affinity	[94]
		Hydrogen sulfide	Fluorescein/dabsyl chloride	0.02 μM	High membrane permeation and compatibility within living cells and biological systems	[95]

Table 3
Recently developed FRET-based biosensors for *in vivo* imaging.

Imaging Principle	Transfection mechanism	Donor-Acceptor	Host-Site	Target	Dynamic detection range	LOD	Property	Ref.
Time-lapse FRET imaging	Virus-associated transfection	CFP/YFP	Transgenic Drosophila-olfactory system, Transgenic mouse-visual cortex	Acetylcholine neurotransmitter	10 nM–100 μM	–	EC50–0.7 μM Sensitivity, ligand specificity, photostability, and feasible imaging of cholinergic signals *in vitro*, ex vivo, and *in vivo*	[109]
			Mice	Potassium	0.37–0.47 mM	0.42 mM	Dynamic quantification of Potassium variations	[110]
		Different fluorescent proteins	Mice-Hippocampus and visual cortex	Neuronal glucose	0.7–2.5 mM	0.4–2 mM	Stability, quantification of glucose in awake mice	[111]
Near-infrared *in vivo* imaging	Intravenous injection	bi-phenyl triazole/ Cy5.5	Mice model of osteoarthritis-	Matrix metalloproteinase 13	–	–	High catalytic efficiency (kcat/ KM = 6.5 × 105 m−1 s−1) and enhanced selectivity for MMP-13	[112]
		Cy5.5 - SQCy7.5	Mice- liver	Drug NPs	2–4 mg mL^{-1}	–	Evaluating the risk of hepatic accumulation of Squalene Prodrug Nanoparticles	[113]
	Viral transfection	Different fluorescent proteins	Transgenic mouse, forebrain excitatory neurons	Calcium	0–39 μM	–	Hybrid photoacoustic and fluorescence microscopy	[114]
Intravital Imaging	Targeting vector generated by inserting a lox-stop-lox transgene	EGFP/mRFP	Transgenic mice	RhoA signaling	–	–	Pre-clinical imaging in normal or disease conditions	[115]
Ratiometric FRET imaging	Biosensor encoding plasmid transfection	CFP/YFP	Live yeast cells	Glutathione	0–10 mM	5.0 mM	Non-invasive, selective, and specific detection of Reduced glutathione low detection limit and real-time cytosolic monitoring	[116]

investigated by a genetically encoded FRET-based biosensor. The biosensor was made of a specific peptide, labeled with a CFP at N-terminus and a YFP (YPet) at C-terminus. In the presence of PSA, intact structure of the biosensor was cleaved and FRET was disrupted. The biosensor represented a 400% change in FRET efficiency in the presence of 1 μg ml^{-1} of PSA [5].

2.2. Molecular detection

FRET-based biosensors are beneficial in determining pivotal points of pathophysiological states as well as illuminating underlying mechanism of disease at molecular scales [82]. Several neurological diseases including human immunoglobulin light chain amyloidosis, Parkinsons', Alzheimers', and Huntingtons' diseases are associated with formation of amyloid fibrils known as plaques [14,83]. Identification of protein folding at early stages is complicated due to heterogeneity and transient nature of aggregates [84]. Several FRET-based biosensors have been developed to obtain clear insights into structural rearrangements, folding, and interactions of proteins [13,85,86]. For instance, in a previous study, folding process of a multi-domain protein, bovine serum albumin (BSA) was investigated through a two-step assay; first, occurrence of FRET was assessed between donor-labeled tryptophan residues and Cys-34 of BSA domain I labeled with IAEDANS (N (Iodoacetaminoethyl)-1-naphthylamine-5-sulfonic acid) acceptor. Second, solvation dynamic of BADAN (6-Bromoacetyl-2-dimethylaminonaphthalene) probes was analyzed during covalent binding with free Cys. The initial compaction in BSA probe was detected after incubation of crowding agents (Dextran 6, 40, 70, and Ficoll 70). At initiation of folding, FRET

Table 4
Recently developed FRET-based immunosensors.

Detection mechanism	Analyte	Donor/Acceptor	linker	Linear range of detection	LOD	Property	Ref.
Immunocomplex formation	*Vibrio cholerae*	CdTe QDs/AuNPs	OmpW antigen	2–10 nM	2 nM	No washing required, simplicity, fast detection	[125]
	Campylobacter jejuni	GQD/GO	Polyclonal Antibody	10–10^6 CFU	PBS 10 CFU mL^{-1} Poultry liver 100 CFU mL^{-1}	High specificity, Fast detection	[126]
	Escherichia coli	QDs/AuNPs	Bacterial cellulose	10–10^8 CFU mL^{-1}	100 CFU mL^{-1}	Feasibility of the immunosensor in the real matrix of booth solid and aqueous samples	[127]
	Para thyroid hormone (PTH) 1–84 antigen	Green CdTe QDS/ Red CdTe QDs	Glass layer	0.01–0.08 ng mL^{-1}	3 pg mL^{-1}	Fast and accurate detection, simple perform and storage	[128]
Competitive and homogeneous immunoassay	Ochratoxin A	QDs of two size	Nanobody	0.05–10 ng mL^{-1}	5 pg mL^{-1}	Ultrasensitive and rapid detection/decreased fluorescence intensity at molar ratio exceeded 10 ng mL^{-1}	[121]
	Fusarium fungi	QDs/AuNPs	Deoxynivalenol	0–10 ng ml^{-1}	28 μg kg^{-1}	One-step, fast responsive, and simplicity, and homogenous assay	[129]
Functionalized antibody-antigen reaction	Avian corona virus	MoS_2/Fluorescent dye	Cotton thread-based microfluidic platform	10^2–10^6 EID50. mL^{-1}	4.6 × 10^2 EID5.mL^{-1}	Low cost, rapid and sensitive detection	[130]
	Cardiac troponin T	Carbon dots/MoS_2	Anti-cTnT	0.1–50 ng. mL−1	0.38 ng mL^{-1}	High sensitivity, rapid and accurate detection/Poor properties of carrier transportation	[131]
Sandwich co-hybridization	Cardiac troponin I	Curcumin ethanol, MoS_2	Nanoprobe	0.0005–5 ng·mL^{-1}	0.5 pg·mL^{-1}	Biocompatibility, High adsorption capacity	[132]
Sandwich co-hybridization of labeled antibodies and target	CA 15-3 tumor marker	Carbon dots/ AuNPS	CA15-3 antibod/ PAMAM-Dendrimer	1.1–16 μU. mL^{-1}	0.9 μU. mL^{-1}	High specificity and selectivity for MDA-MB-231 cells concentrations	[124]
Enzymatic catalysis of the substrate	Procalcitonin	β-CD-ZnS QDs/3-hydroxyflavone	Amp cephalosporinase	0.1–70 ng mL^{-1}	0.03 ng mL^{-1}	Ultrasensitive and accurate detection, Long-term stability of the enzyme	[64]

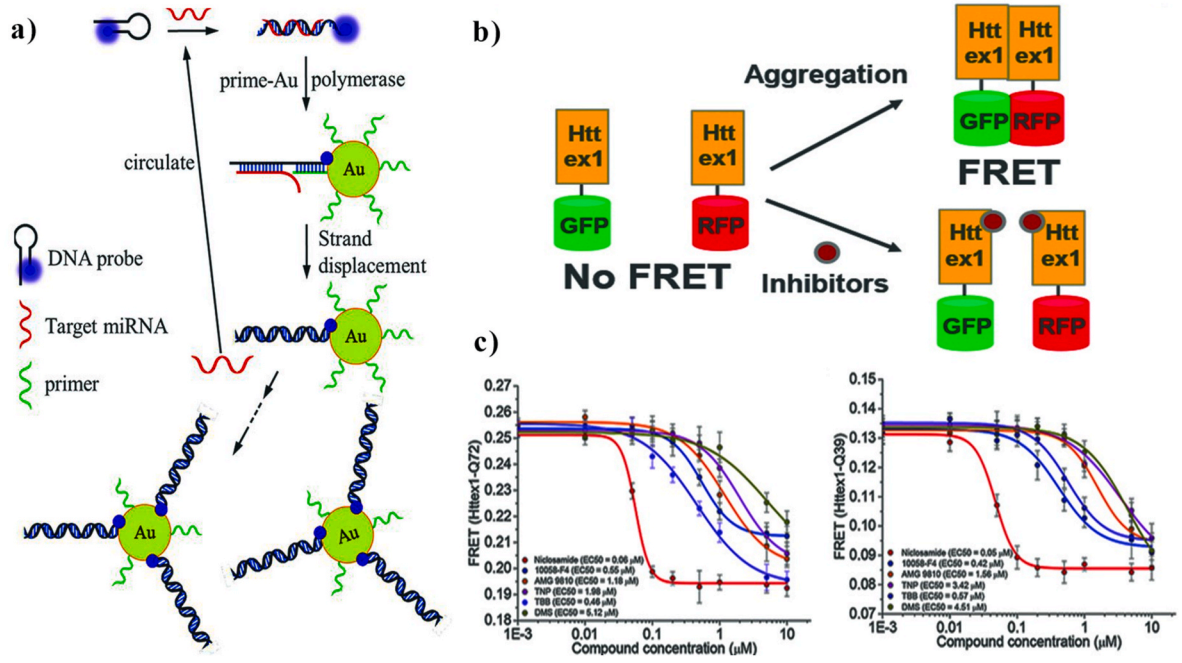

Fig. 2. FRET-based biosensors for cellular and molecular detection. **a)** Schematic diagram of miRNA detection based on signal amplification through target cycling reaction and quenching efficiency of AuNPs. In the presence of target miRNA, structure of the Cysteine 5-labeled stem-loop DNA probe was opened leading to hybridization of the AuNP-labeled primers and fluorescence quenching through FRET. Continuous strand displacement and duplex amplification by the released miRNA decreased fluorescence intensity [79], with permission obtained from the Royal Society of Chemistry. **b)** Schematic representation of FRET-based biosensor consisting of GFP/RFP-labeled huntingtin exon 1 protein (Httex1) designed for determining aggregation of Httex1 inhibitors. Formation of Httex1 protein aggregates led to development of acceptor red fluorescent signal, while inhibitor treatment resulted in the attenuated FRET. **c)** A dose-dependent decrease was observed in fluorescence signal intensity in the case of Httex1 inhibitors' aggregation [88], with permission obtained from the ACS publications. (For interpretation of the references to color in this figure legend, the reader is referred to the Web version of this article.)

efficiency was low (~18%), while complete folding of domain I resulted in donor-acceptor proximity and increased FRET efficiency. Solvent correlation analysis of BADAN in BSA-BADAN revealed that this domain becomes rigid during the initial phase of aggregation. However, its flexibility was increased until the final aggregation [87]. On the other hand, accurate analysis of proteins' structural modifications allows for identification of effective molecules to inhibit protein misfoldings. In this respect, in a prior research, a FRET-based biosensor was used to discover reproducible small molecules (hits) capable of inhibiting huntingtin exon 1 (Httex1) aggregation. The biosensor could monitor Httex1 folding in neuroblastoma and human embryonic kidney 293 (HEK 293) cells. Six hits were identified during high-throughput screening of pharmacologically active compounds' library. These molecules strongly attenuated FRET with 50% effective concentration (EC50) values ranging from 0.05 to 5 μM (Fig. 2b). Aggregation of Httex1 resulted in occurrence of FRET, while in the presence of hits, FRET efficiency was reduced in a dose-dependent manner (Fig. 2c). Ultimately, niclosamide was introduced as the most efficient hit to inhibit Httex1 aggregation [88]. In addition, in another study, a biosensor was developed to detect small molecules capable of modulating skeletal muscle channel isoform (RyR1) interactions with FK506 binding protein 12.6 and calmodulin. Dysregulation of RyR1 channels results in Ca^{2+} leakage associated with neurodegeneration, diabetes, and severe skeletal and cardiac myopathies. FRET efficiency was increased in the presence of RyR1 inhibitors in a dose-dependent manner. Chloroxine and myricetin were identified as small molecules which the reduced Ca^{2+} leakage from RyR1 in human embryonic kidney 293 cells [12].

3. FRET-based biosensor for cell-based imaging *in vitro*

Multiplexing approaches have provided expedient analytical tools for elucidation of cellular and molecular assemblies (54). FRET-based biosensors are effectually used for quantitative and non-invasive *in-vitro* imaging and cell-based analysis of biological compounds [90,91] (Table 2).

Regarding sensitivity of serine proteases to metal ions, in a study, a FRET-based biosensor was used to monitor the influence of Zn^{2+} and Cu^{2+} on activity of high-temperature requirement A (HtrA) *in vitro*. HtrA is a serine protease expressed in *Helicobacter pylori*, which could cleave surface proteins of gastric epithelial cells and disrupt epithelial integrity. The peptide consisted of a 2-aminobenzoyl reporter at the N terminal, a 3-nitro-tyrosine Y quencher, and an optimized AQRVAF sequence containing a hydrolysis site of HtrA. The results indicated that low concentrations of Zn^{2+} (649.5 nM) and Cu^{2+} (295.4 nM) (50% inhibitory concentration) efficiently inhibited HtrA activity. Thus, the designed FRET peptide introduced a novel method to evaluate metal ion-dependent protease inhibitors,which could prevent bacterial growth, survival, and pathogenesis [96]. In a recent study, human transferrin receptor 1 (TfR1) was directly labeled with a folic acid-derived FRET probe for accurate screening of fR1-mediated endocytosis. The probe enabled live-cell imaging of redox activity during endocytosis in HeLa cell endosomes. Reducing environment of endosomal compartments caused probe cleavage and subsequently, attenuated FRET. The results supported principle of receptor-ligand interactions as an important strategy for the targeted drug delivery [97]. For high spatiotemporal imaging, FRET-based biosensors could reach subcellular domains via nanocarriers,such as lipid rafts [24]. Besides, conjugation of fluorescent organic NPs with FRET probes like quatsomes has significantly enhanced photophysical and physicochemical properties of FRET probes and preserved their integrity during membrane internalization [25]. However, single-photon emission probes have been shown to encounter several challenges for cell-based imaging *in vitro* including low stability, intercellular aggregation, fluctuation of radiation light, microenvironment problems, and systematic errors [20]. Ratiometric imaging relies on analyte-induced changes in emission intensity of two or more fluorescence signals that could be simultaneously measured at different wavelengths and calculated individually [98]. Accordingly, in a research, a ratiometric FRET probe named as CP-K was designed to monitor Cys derivatives in mitochondria of MCF-7 breast cancer cells. CP-K was composed of a coumarin donor and N-ethyl-2-styrylquinolinum acceptor exhibiting high sensitivity toward SO_2 metabolites with LOD of 26.3 nM. Addition of 0–10 equiv. of HSO_3^- was accompanied by an obvious decrease in fluorescence absorbance (from 483 to 150 nm) and a distinct change in signal color (from orange-red to yellow). The results indicated high permeability and photostability of CP-K in a complex physiological environment. Consequently, the biosensor allowed for colorimetric naked-eye detection of endogenous sulfite derivatives in live cells [23]. Recently, in another research, an NP-based FRET biosensor was successfully designed to monitor caspase-9 activity during cisplatin-induced apoptosis in MG-63 and SW480 colorectal tumor cells. The biosensor comprised of a peptide containing a specific motif (LEHD) as caspase-9 cleavage site and was functionalized by UCNP@silica donor and Cy5 acceptor. As demonstrated in Fig. 3a, in the presence of caspase-9, Cy5 was detached from UCNP@SiO_2 surface, and donor emission was restored. It was reported that cisplatin-treated MG-63 cells demonstrated higher levels of caspase-9 activity compared to SW480 cells in the same condition. Moreover, donor signal intensity represented a linear dependency on amount of MG-63 cells with LOD of 675 cells [99]. In a recent study, naphthalimide (Np) and rhodamine (Rh) were used as FRET pairs to construct ratiometric probes for selective detection of lysosomal peroxynitrite ($ONOO^-$) in HeLa cells. The NpRh-ONOO biosensor offered rapid (<10 s) and quantitative detection of $ONOO^-$ in a wide range (0–8.0 μM) with high sensitivity (LOD of 3.33 nM) [100]. Ghosh et al., fabricated a FRET-based biosensor using pH-sensitive fluorophores for ratiometric imaging of pH changes within a single cell. The biosensor incorporated UCNP and mOrange FP and represented ~20% of FRET efficiency at physiological pH (7–7.5). Ratiometric properties of this biosensor changed linearly in response to pH changes (3.0–8.0). The pH of intracellular compartments was accurately determined by this biosensor in HeLa cells. Designed FRET probes represented high photostability, sensitivity, and non-toxicity, with minimum background autofluorescence [101]. In another study, a ratiometric FRET probe named as RhChr was developed for *in vitro* imaging of xanthine oxidase (XOD) activity and quantification of hydroxylamine (HA). The biosensor possessed the least cytotoxicity in HepG2 cervical cancer cells and represented a linear relation between HA concentration (0–80 μM) and FRET efficiency with LOD of 2.16 μM [102]. Likewise, in a study, a FRET-based biosensor was established for ratiometric imaging of nitroreductase (NTR) as a biomarker of hypoxia in A549 lung tumor cells. This biosensor acted based on occurrence of both FRET and photoinduced electron transfer (PET). The 1,8-naphthalimide (NA) was used as acceptor and its linked form to poly(fluorene-*co*-phenylene) (PFP-NA) was used as donor. According to Fig. 3b, in normal conditions, fluorescence signal of NA (FRET) was quenched through PET, while during cellular hypoxia, the produced NTR led to occurrence of FRET (>54 folds) by blocking PET. This structure detected NTR with LOD of 19.7 ng mL^{-1} and could provide effective guidance for tumor therapy [103]. Application of FRET-based biosensors for visualization of intracellular signaling pathways has provided a high throughput platform for accurate detection and therapeutic outcomes. In a previous study, the effect of kinase inhibitors (KIs) on extracellular signal-regulated kinase (ERK) and AKT signaling pathway was investigated in triple-negative breast cancer cell lines (HCC1806 and Hs578T) by FRET-based biosensors. The biosensors were fabricated with CFP-YPF -labeled peptide substrates and the correlation between KIs and proliferation was determined in both signaling pathways [104]. Furthermore, in a research, a ratiometric FRET probe was designed for live-cell screening of endogenous hydroxyl radicals in zebrafish. The probe was labeled with Rho and N_2O-type structure named as Bobpy as donor and acceptor, respectively. According to donor stronger emission in hydrophobic environment and signal-to-noise ratio (SNR) of 3, the probe was capable of membrane-organelle targeted imaging. As represented in Fig. 3c, the biosensor could attack ·OH released either from the

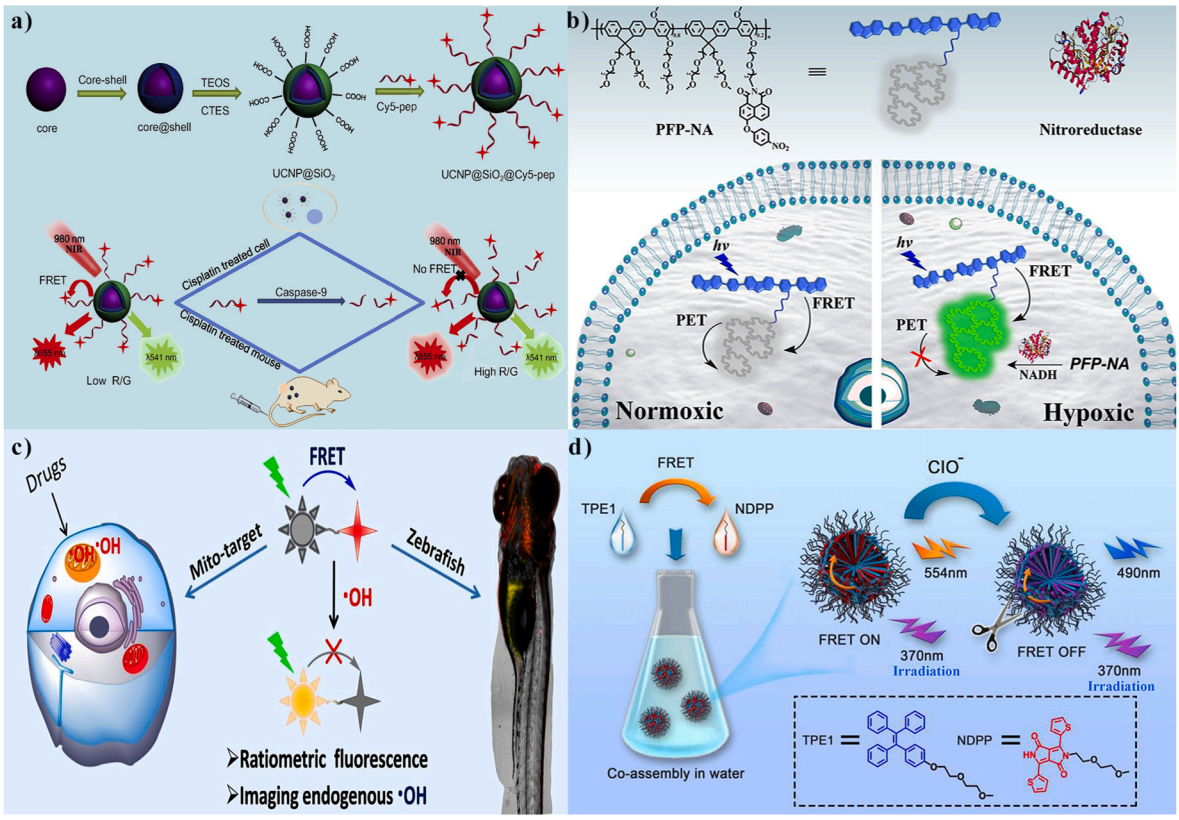

Fig. 3. FRET-based biosensors for *in vitro* imaging. **a)** Schematic illustration of an upconversion NPs (UCNP@SiO_2)-based FRET biosensor developed to monitor the Caspase-9 activity both *in vitro* and *in vivo*. A Cysteine 5- labeled peptide containing caspase-9 cleavage site (LEHD) was conjugated with UCNP@SiO_2 and was able to quench red emission of upconversion luminescence (UCL). The caspase-9 activity resulted in LEHD cleavage and recovery of UCNP@SiO_2 red emission. The caspase activity levels were determined by quantification of red to green signal ratio, with permission from the journal (license number: 5113710238884) [99]. **b)** FRET-based biosensor comprised of water-soluble 1,8-naphthalimide (NA) conjugated polymers (PFP-NA) for detection of nitroreductase (NTR) during hypoxia in tumor cells. In normal conditions, FRET between NA and PFP was simultaneously quenched by the photoinduced electron transfer (PET) effect between them, while in the presence of NTR, the reduced nitro group led to blockage of PET and recovery of FRET between NA and PFP, with permission from the journal (license number: 5113710961168) [103]. **c)** Ratiometric imaging of hydroxyl radicals in zebrafish by rhodamine (Rho)-labeled N_2O-type FRET-based biosensor. The reaction between endogenous hydroxyl radicals and the designed biosensor in mitochondria led to separation of Rho (donor) and the N_2O-type structure (quencher) and recovery of the donor signal [105], with permission obtained from the Royal Society of Chemistry. **d)** Schematic illustration of tetraphenylethene (TPE)/diketopyrrolopyrrole (NDPP) pairs co-assembly in water to construct biosensor for ratiometric imaging of hypochlorite in live cells. NDPP acted as a reactive unit for hypochlorite (ClO^-) and FRET between TPE donor and NDPP acceptor was disrupted upon ClO^- binding to NDPP, with permission from the journal (license number: 4990260818237) [22]. (For interpretation of the references to color in this figure legend, the reader is referred to the Web version of this article.)

Fenton reaction or drug activation in mitochondria. The biosensor was suggested as an efficient and sensitive tool for live-cell imaging and specific detection of ·OH with LOD of 0.68 μM [105]. Intracellular accumulation and signal overlap in ratiometric probes could limit their application for cellular imaging. In this regard, aggregation-induced emission (AIE)-based FRET probes have been developed to enhance fluorescence emission intensity at the aggregated state with no aggregation-caused signal quenching [106]. In a related study, an AIE-based FRET biosensor was established for imaging of hypochlorite (ClO^-) in HeLa cells. The probe was labeled with amphiphilic tetraphenylethene (TPE1) donor and amphiphilic diketopyrrolopyrrole acceptor assembled to a hybrid NP. This probe represented high stability, simple construction, and good solubility in comparison with the existing single probe FRET systems. Low concentrations of ClO^- (LOD of 105 nM) resulted in complete recovery of TPE1 emission. This hybrid biosensor could successfully image ClO^- in HeLa cells due to bright fluorescence, selective targeting, and high permeability through a live cell membrane (Fig. 3d) [22].

4. FRET-based biosensors for *in vivo* tissue imaging

Application of FRET-based biosensors for tissue-depth and *in vivo* imaging has successfully enabled spatiotemporal visualization of molecular compounds and multiplexed imaging of cellular processes in living models (Table 3) [107,108].

Accordingly, in a study, apoptosis was visualized at single-cell resolution using an engineered FRET-based biosensor (Fig. 4a). The biosensor comprised of a specific peptide containing caspase cleavage site (DEVD) and CFP-YFP as FRET pair, and was transgenically expressed in skin cells of zebrafish (Fig. 4b). In physiological conditions, a green fluorescent signal was acquired while caspase-3 activity during apoptosis switched signal to blue (Fig. 4c). Using time-lapse FRET imaging, the biosensor revealed that caspase-3 was activated within 3 min of apoptosis induction either through ultraviolet (UV) irradiation or during development process of zebrafish. Moreover, it was reported that apoptosis could be completed in about 30 min after caspase-3 activation. The results confirmed occurrence of apoptosis in the skin covering zebrafish head, eyes, and yolk at all stages of normal growth (Fig. 4d) [21]. Regarding the critical effect of Ca^{2+} on development and function of immune cells, a FRET-based biosensor was developed in a study to monitor Ca^{2+} signaling during immune responses. FRET-based Ca^{2+} indicator was transgenically expressed in immune and nerve cells of transgenic mice. The biosensor included a double-chromophore indicator Yellow cameleon 3.60 (YC3.60) employing CFP and Venus 6 as FRET pair that enabled intravital spatiotemporal analysis of Ca^{2+} signaling in lymphoid tissues [117]. Recently, in

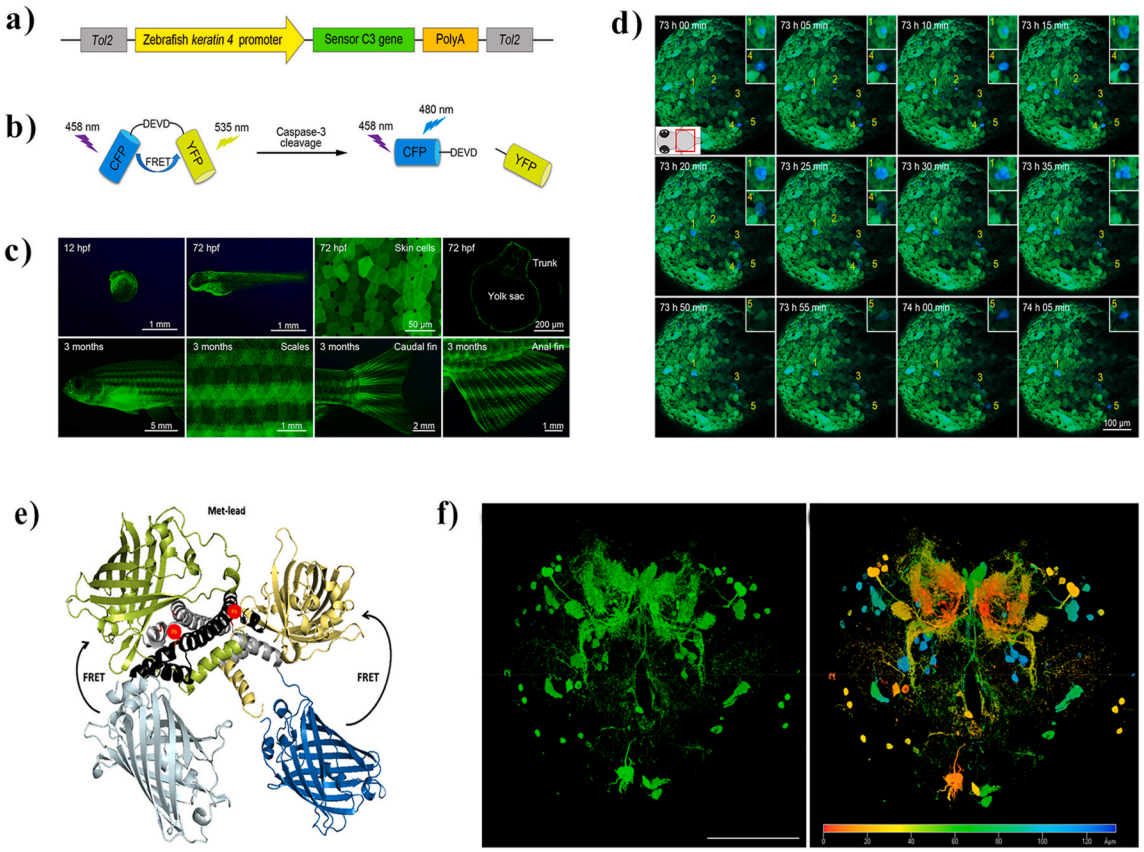

Fig. 4. FRET-based biosensors for *in vivo* imaging. **a)** Schematic representation of FRET-based biosensor (C3) for real-time monitoring of caspase-3 activity. The main components of transposon encoding C3 used to generate transgenic zebrafish through the Tol2-mediated gene transfer. **b)** The biosensor comprised of a specific peptide containing caspase-3 cleavage site (DEVD) and CFP/YFP as FRET pair. **c)** Transgenic zebrafish (krt4: sensor C3) expressed C3 at different stages of development in different regions. **d)** Real-time tracking of skin cells' apoptosis in live zebrafish during natural process of development acquired by time-lapse FRET imaging [21], with permission obtained from the ACS publications. **e)** Schematic illustration of the biosensor structure designed to detect Met-lead. The biosensor was composed of a YFP/CFP-labeled dimer protein (PbrR) serving two binding sites for lead ions. Upon binding of lead, conformational changes in PbrR resulted in FRET between YFP and CFP. **f)** Optical images of transgenic Drosophila brain in the presence of lead ions were acquired with green fluorescent signals and in-depth color imaging [118], with permission obtained by a Creative Common CC BY license. (For interpretation of the references to color in this figure legend, the reader is referred to the Web version of this article.)

an investigation, a FRET-based biosensor (Booster-PKA) was designed for *in vivo* monitoring of protein kinase A (PKA) activity. The biosensor was genetically expressed in transgenic mice and consisted of an FHA1 phosphothreonine-binding domain, a flexible linker peptide, a sensor domain, mKOκ donors, and mKate acceptors. Transgenic mice were generated by Tol2-mediated gene transfer and grew normally with no signs of external or internal malformations. The Booster-PKA represented a dose-dependent detection of cyclic adenosine monophosphate (cAMP) analog (forskolin) in a linear range (0.28–26 μM) with LOD of 1.74 μM. *In vivo* imaging of liver, kidney, and colon in the generated transgenic mice validated the biosensors' ability in monitoring PKA activation in the presence of cAMP [26]. According to the harmful effects of heavy metal ions, accurate determination of these ions in circulation system is of great importance. In this regard, in a previous research, a FRET-based biosensor was designed to determine blood level of lead and illuminate underlying mechanism of lead-related toxicity. As shown in Fig. 4e, the biosensor incorporated a specific PbrR protein as a lead binding site labeled with YFP-CFP and was transgenically expressed in Drosophila. Upon binding of lead, conformational changes in the PbrR-sensing domain brought the donor and acceptor to proper proximity for occurrence of FRET. The designed system measured lead content inside living cells with LOD of ~10 nM (Fig. 4f) [118]. Although, several *in vitro* studies have been accomplished to investigate AMP-activated protein kinase (AMPK) regulation, exact details of this process have remained unclear. Therefore, in another research, a FRET-based biosensor was fabricated for *in vivo* imaging of AMPK regulation. AMPK is a cellular energy regulator effectively targeted in treating type 2 diabetes and obesity. Transgenically expressed biosensor named as AMPKAR-EV was labeled with CFP-YFP, incorporating a kinase substrate peptide and a flexible linker (EV). AMPKAR-EV efficiently determined the role of liver kinase B1 (LKB1) as an AMPK stimulator and monitored drug-induced regulation of AMPK activity *in vivo*. The results demonstrated metformin-induced activation of LKB1 in transgenic mice with EC50 ~10 mM, while AICAR (an AMP analog) stimulated activation of AMPK in muscle with EC50–0.5 mM. In addition, organ-specific activation of AMPK and heterogeneity of drug-induced responses were confirmed in this assay [27]. In a prior research, ratiometric *in vivo* detection of ovarian cancer biomarker, γ-glutamyl transpeptidase (GGT), was performed by a FRET-based biosensor (Py-GSH). The biosensor comprised of a GGT responsive probe (GSH) directly labeled with fluorescent Pyronin B, which emits a strong red signal. In the presence of GGT, γ-glutamyl cleaved the Py-GSH followed by fast intramolecular rearrangement that consequently resulted in bright green emission. The Py-GSH potential for GGT detection was investigated in mouse models of solid ovarian tumors (by subcutaneous injection) as well as metastatic intra-abdominal tumors (by intraperitoneal injection). Obvious optical changes in fluorescence signals in stained tumor tissues indicated the biosensors' efficiency in rapid and naked-eye detection of cancerous tissues. Ultimately, Py-GSH was used for POC detection of tiny malignant tumors during clinical resection of meta static ovarian tumors [28]. In a recent study, the impaired nitric oxi

de (NO)/cyclic guanosine monophosphate (cGMP)/phosphodiesterases (PDE) 2 signaling was investigated in a rat model of failing cardiomyocytes using a FRET-based biosensor. Following heart failure, the decreased levels of cGMP led to negative cGMP-to-cAMP cross-talk depending on the weakened PDE 2. The biosensor provided direct monitoring of cardiomyocyte b3-adrenoceptors (b3-ARs) associated with cGMP production, accurate sub-membrane localization of b3-ARs, and altered b3-AR/cGMP signaling in failed cardiomyocytes. Using scanning ion conductance microscopy, the biosensor identified major localization of functional b3-ARs on cardiomyocytes T-tubules of healthy rats [119]. Despite increasing number of the established FRET-based biosensors, their practical application for *in vivo* imaging is limited due to several issues. For instance, inadequate expression of the biosensor, poor biocompatibility, immunogenicity, and limited spatial resolution due to the biosensor size and location are some challenges of FRET-based imaging *in vivo* [120].

5. FRET- based biosensors for *in vitro* immunoassays

FRET-based immunosensors have integrated FRET sensitivity with specificity of immunosensors [121]. Fabrication of FRET-based immunosensor mainly relies on the used linking method including 1-Ethyl-3-(3-dimethylaminopropyl) carbodiimide (EDC)/sulfo-N-hydroxysuccinimide (NHS), dicyclohexyl carbodiimide (DCC)/NHS, and biotin/streptavidin reactions [121–124]. Several FRET-based immunoassays have been successfully designed for direct and rapid detection of various targets including viruses, antigens, hormones, toxins, cancer biomarkers, and protein complexes (Table 4).

FRET-based immunosensors possess unique properties,such as high stability, specificity, and ratiometric signals [29]. Interestingly, integration of immunosensors with FRET-based imaging and targeted drug delivery systems has greatly influenced POC diagnosis and treatment strategies [131–133]. As a proof of concept, in a study, parathyroid hormone (PTH) 1–84 antigen in human blood samples was detected with LOD of 3 pg mL^{-1} using a FRET-based immunosensor. The biosensor comprised of 2-mercaptopropionic acid stabilized two-color CdTe-QDs linked with PTH 1–84 antigen and FRET between CdTe-QDs resulted in accurate detection of PTH 1–84 antigen in UV light region. The red CdTe QDs@PTH 1–84 antigen and label-free target antigens were competitively bound to green CdTe-QDs@PTH 1–84 antibody. The green fluorescent signal was gradually enhanced by increasing concentration of target PTH 1–84 antigen, which consequently resulted in change in fluorescence color from red to green. The biosensor provided a key tool for rapid PTH detection in related disorders including breast and lung cancers, chronic kidney disorders, and cardiovascular diseases [128]. FRET-based immunosensors are expected to enhance performance, sensitivity, and stability of the current immunoassays,such as ELISA and nanoenzymes along with resolving their limitations including single-mode readout, possibility of false-positive results, insufficient sensitivity to low concentrations of analytes, and enzyme vulnerability [64,134]. Accordingly, in a research, a pH-responsive FRET-based immunosensor was established for dual-readout fluorescence and colorimetric detection of cardiac troponin I (cTnI) as a biomarker of acute myocardial infarction. The biosensor contained curcumin (CUR) as a pH indicator (donor) immobilized on three-dimensional MoS_2 nanoflowers (3D-MoS_2 NFs) (acceptor) that could quench the CUR fluorescence signal through FRET. For incorporating smart drug delivery systems (DDS) with ELISA (DDS-ELISA), cTnI antibodies were immobilized on MoS_2 NFs through carbodiimide conjugation. In the presence of cTnI in basic pH, co-hybridization of cTnI antibodies resulted in formation of sandwich immunosensor. Consequently, hydrophobic CUR turned into hydrophilic salt and was separated from MoS_2 NFs, which led to recovery of CUR yellow signal (Fig. 5a). The biosensor enabled naked-eye detection of cTnI in a linear range of concentration (0.0005–5 ng·mL^{-1}) with LOD of 0.074 pg·mL^{-1} and 0.5 pg·mL^{-1} for fluorescence and colorimetric readout, respectively [132]. Similarly, in a study, cardiac troponin T (cTnT) was detected by a FRET-based immunosensor comprised of carbon Dots/MoS_2 nanosheets and cTnT antibodies. In the presence of cTnT, formation of sandwich immune structure (anti-cTnT/cTnT) resulted in separation of CDs from MoS_2 and fluorescence signal of CDs was recovered. This immunosensor represented a linear response to cTnT concentration in the range of 0.1–100 ng mL^{-1} with LOD of 0.12 ng mL^{-1} [131]. In a recent study, a FRET-based biosensor was established for rapid and sensitive detection of alpha-fetoprotein (AFP), which is an important biomarker of hepatocellular carcinoma. The biosensor comprised of an AFP-specific aptamer labeled with QD donors and an anti-AFP monoclonal antibody labeled with AuNP acceptors. In the presence of target AFP, bio-affinity between donor-labeled aptamer and acceptor-labeled antibody resulted in fabrication of QDs-AFP-AuNPs sandwich structure and occurrence of FRET due to donor-acceptor proximity. This structure detected AFP in human serum samples with LOD of 400 pg mL^{-1} [135]. Owing to advances in manipulating FPs, FRET-based biosensors have provided a powerful tool in the context of drug evaluation and targeted therapy [136–138]. Ratiometric screening of drug delivery, monitoring cellular entrance, trafficking and metabolism of the drug, as well as evaluation of cellular sensitivity and responses to drugs are considerably improved by FRET-based immunoassays [139–142]. In this respect, Lee et al., monitored intercellular activity of antibody-drug conjugates (ADCs) using FRET-based immunosensors. Two growth factor receptors, namely HER2 and tomoregulin were targeted by FAM-TAMRA-labeled probes conjugated with maytansinoid DM1cytotoxic agent. The probes were selectively linked with antibodies through thiol-Cys conjugation. Intercellular uptake, trafficking, and processing mechanisms of the ADCs were investigated in the engineered SK-BR-3 breast cancer and PC3 prostate cancer cells expressing cancer-specific HER2 or tomoregulin-2 growth factor receptors. Investigated cells represented limited cytosolic transport of maytansinoid DM1 despite efficient cleavage of the linkers. The results indicated the role of cellular background in trafficking of ADCs [143]. Moreover, in some cases, the use of chemically -labeled antibody-FRET probes could be limited to target organelle or cell line [144,145]. In a research, the inhibitory effect of human endonuclease III and Y-box binding protein 1 (hNTH1−YB1) complex in breast cancer was monitored through a FRET-based immunoassay. Using AlphaLISA to pinpoint regions of hNTH1 and YB1, the biosensor was stably transfected to the MCF-7 breast cancer cells. In addition, potential inhibitors of this complex were identified by screening chemical libraries. Ultimately, the hNTH1−YB1 complex was reported to serve as a target in establishing novel therapeutic components against drug-resistant tumors [30]. Recently, the first FRET-based immunochromatography test strip (ICTS) was successfully designed in a study for colorimetric naked-eye detection of PSA in whole-blood samples. ICTS is a lateral-flow immunochromatographic assay that proves to be one of the most prevalent types of POC detection methods. Fluorometric ICTS incorporated a PSA detection antibody labeled with functionalized coumarin nanoparticle (PCA) donors and PSA capturing antibodies labeled with inorganic quantum nanocrystal (PF-TC6FQ Pdots) acceptors. In addition, immunoglobulin G (IgG) was immobilized on control line of the strip as secondary antibody (Fig. 5b). By adding blood samples, porous membrane selectively blocked the blood cells permitting plasma-serum migration through the strip via capillary flow. In the presence of PSA, formation of antigen-antibodies immune complexes led to occurrence of FRET due to donor-acceptor proximity. Distinctive changes in emission color represented a linear dependency on antigen concentration allowing sensitive naked-eye detection of PSA and quantitative analysis in a dynamic range from 2 to 10 ng mL^{-1} with LOD of 0.32 ng mL^{-1} (Fig. 5c) [146]. Similarly, the first homogeneous FRET-based immunoassay was developed in a previous research for concomitant detection of epidermal growth factor receptor (EGFR) and HER2 in a single sample. The immunosensor incorporated an NHS-functionalized Terbium (Tb) and a maleimide-functionalized QD duplex (Tb-QD). Tb-QD allowed direct comparison of QDs-labeled monoclonal antibodies (cetuximab, pertuzumab, trastuzumab, and matuzumab) and

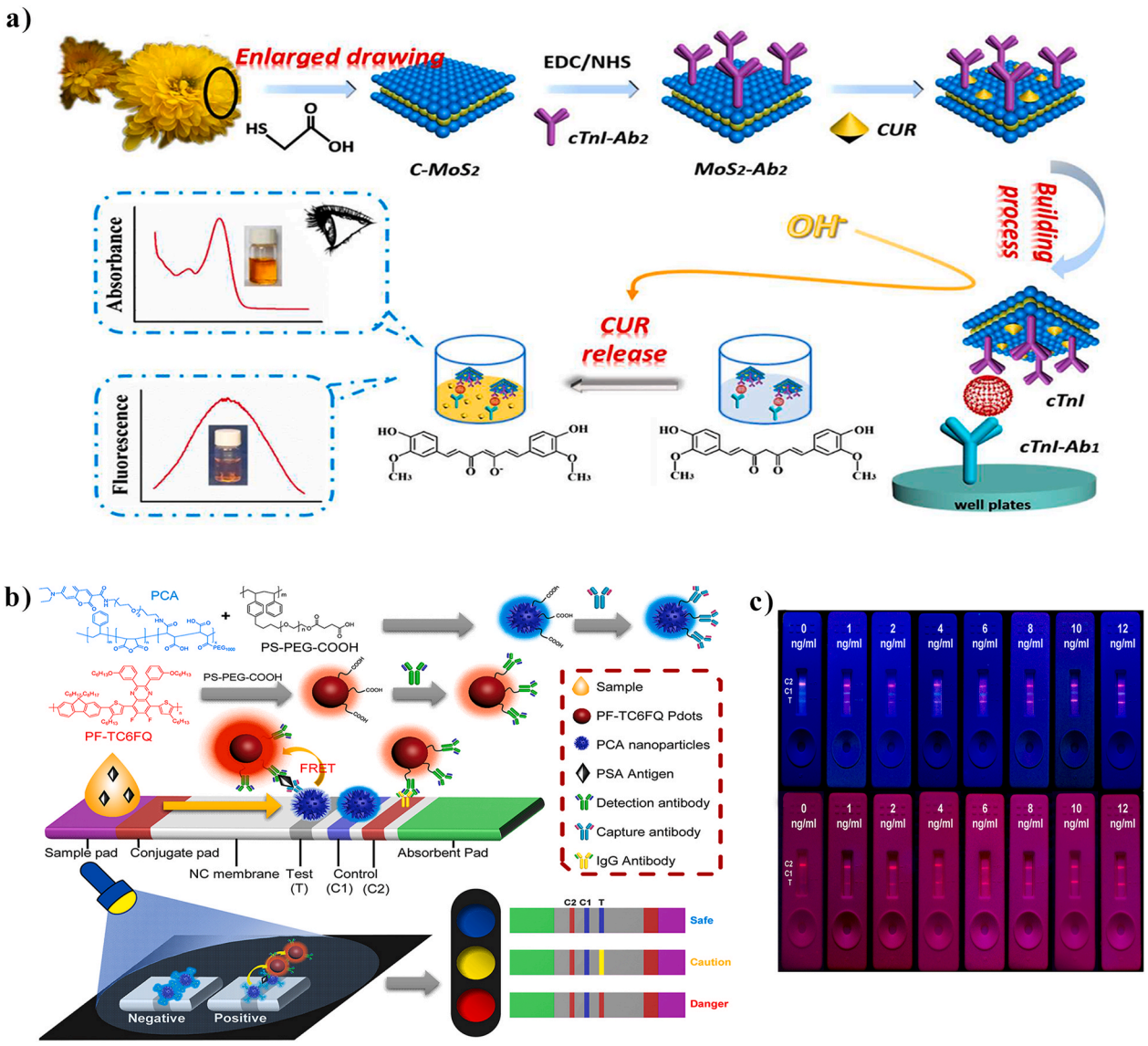

Fig. 5. FRET-based immunosensors. **a)** Schematic diagram of a developed FRET-based immunosensor to integrate drug delivery system (DDS) with inspired enzyme-linked immunosorbent assay (ELISA) (DDS-ELISA) for detection of cardiac troponin I (cTnI). The cTnI antibody was immobilized on a three-dimensional MoS_2 nanoflower (3D-MoS_2 NFs) surface through EDC/NHS- mediated carbodiimide coupling. Hydrophobic curcumin (CUR) was absorbed on MoS_2 NFs and its fluorescence signal was quenched by MoS_2 NFs. Co-hybridization of antibodies with cTnI at basic pH resulted in release of CUR from MoS_2 and restoration of fluorescence signal [131], with permission obtained from the Royal Society of Chemistry. **b)** A FRET-based fluorometric lateral flow immunochromatographic strip (ICTS) designed for colorimetric recognition and quantitative analysis of prostate-specific antigen (PSA) in whole blood samples. In the presence of antigen, co-hybridization of PSA-specific antibodies labeled with COOH functionalized coumarin nanoparticles (PCA) and inorganic quantum nanocrystals (PF-TC6FQ Pdots) resulted in occurrence of FRET and a distinctive change in emission color. **c)** Photographic images and corresponding fluorescence photographs of fluorometric ICTS under 410 nm of UV irradiation using a 600 nm long-pass filter. The biosensor detected PSA in a dynamic range of 0–12 ng mL^{-1} [146], with permission obtained from the ACS publications. (For interpretation of the references to color in this figure legend, the reader is referred to the Web version of this article.)

nanobodies (18A12 VHH, 11A4, EgA1, and EgB4). The biosensor detected nanomolar concentrations of HER2 using oriented 18A12 and 11A4 conjugates (LOD of 8.0 ng mL^{-1}) and EGFR by matuzumab and cetuximab conjugates (LOD of 2.9 ng mL^{-1}). The results confirmed that several parameters including antibody orientation and size, conjugation ratio, antibody non-specific binding, and cross-reactivity could influence conjugation efficiency of FRET pair-antibody and performance of FRET-based immunoassays [147].

6. Conclusion and the future prospective

FRET-based biosensors have provided a quantitative analytical tool to be used in several fields including biomedical applications, pharmacology, toxicology, and food analysis. In the biomedical context, FRET-based biosensors have proved to be effective for achieving the detailed understanding about cellular processes and accurate quantification of the involved small molecules. Spatiotemporal analysis of biomolecule dynamics using distance-dependent FRET-based biosensors could illuminate underlying mechanism of neurodegenerative diseases. Accurate identification of cancer biomarkers, such as miRNAs and tumor-specific antigens has been successfully performed by FRET-based biosensors. Owing to optical properties and low toxicity, FRET-based biosensors are broadly utilized in high throughput and real-time monitoring of cellular processes, such as apoptosis within a live cell, tissue, organism, and also 3D biomimetic systems. Non-invasive and ratiometric FRET imaging (both *in vitro* and *in vivo)* has offered ultrasensitive detection mechanisms along with introducing novel therapeutic prospects. FRET-based immunosensors have offered impressive multiplexing platforms for

biomedical diagnosis due to their simplicity and rapidness, being homogeneous assays, lack of requiring washing steps, and low cost. Accordingly, FRET-based biosensors could promise a novel perspective for real-time-whole-body screening, POC identification of tiny metastatic tumors, targeted cancer therapy, and imaging-based surgery. Despite various advantages, unavoidable SNR, inadequate fluorescence resolution, and low stability of reagents are some challenges of FRET-based biosensors that require further studies. Moreover, relatively large size and high cost of fluorescent tags could restrict design of FRET-based biosensors as well. Therefore, additional investigations are required with a major focus on improving these limitations and enhancing reaction specificity. Manipulating surface properties of affordable NPs and using alternative tags with fluorescent potential, such as carbon-based composites could be considered in designing FRET-based biosensors.

Author contribution

Mahsa Imani: conceptualization, investigation, writing – original draft, writing – review & editing. Nasrin Mohajeri: conceptualization, project administration, software, writing – review & editing. Mojgan Rastegar: visualization, project administration. Nosratollah Zarghmi: supervision, funding acquisition.

Declaration of competing interest

The authors declare that they have no known competing financial interests or personal relationships that could have appeared to influence the work reported in this paper.

Acknowledgment

The authors would like to thank Tabriz University of Medical Sciences (TUOMS) for financially supporting this project. This study was partly taken from a MSc thesis (IR.TBZMED.REC.1397.1005) that performed at the Faculty of Advanced Medical Sciences of Tabriz University of Medical Science, Tabriz, Iran.

References

[1] A. Kaur, S. Dhakal, Recent applications of FRET-based multiplexed techniques, TrAC Trends Anal. Chem. (Reference Ed.) 123 (2020), https://doi.org/10.1016/j.trac.2019.115777.
[2] S. Bhuckory, J.C. Kays, A.M. Dennis, In vivo biosensing using resonance energy transfer, Biosensors 9 (2019), https://doi.org/10.3390/bios9020076.
[3] L. Wu, C. Huang, B.P. Emery, A.C. Sedgwick, S.D. Bull, X.P. He, H. Tian, J. Yoon, J.L. Sessler, T.D. James, Förster resonance energy transfer (FRET)-based small-molecule sensors and imaging agents, Chem. Soc. Rev. 49 (2020) 5110–5139, https://doi.org/10.1039/c9cs00318e.
[4] G. Bunt, F.S. Wouters, FRET from single to multiplexed signaling events, Biophys. Rev. (2017), https://doi.org/10.1007/s12551-017-0252-z.
[5] H. Yao, L. Wang, J. Guo, W. Liu, J. Li, Y. Wang, L. Deng, M. Ouyang, Genetically encoded FRET biosensor detects the enzymatic activity of prostate-specific antigen, MCB Mol. Cell. Biomech. (2020), https://doi.org/10.32604/mcb.2020.09595.
[6] C.H. Lo, N.K. Pandey, C.K.W. Lim, Z. Ding, M. Tao, D.D. Thomas, R. Langen, J. N. Sachs, Discovery of small molecule inhibitors of huntingtin exon 1 aggregation by FRET-based high-throughput screening in living cells, ACS Chem. Neurosci. (2020), https://doi.org/10.1021/acschemneuro.0c00226.
[7] X. Zhang, Y. Hu, X. Yang, Y. Tang, S. Han, A. Kang, H. Deng, Y. Chi, D. Zhu, Y. Lu, FÖrster resonance energy transfer (FRET)-based biosensors for biological applications, Biosens. Bioelectron. 138 (2019) 111314, https://doi.org/10.1016/j.bios.2019.05.019.
[8] A.S. Klymchenko, Solvatochromic and fluorogenic dyes as environment-sensitive probes: design and biological applications, Acc. Chem. Res. 50 (2017) 366–375, https://doi.org/10.1021/acs.accounts.6b00517.
[9] H. Zhu, J. Fan, J. Du, X. Peng, Fluorescent probes for sensing and imaging within specific cellular organelles, Acc. Chem. Res. 49 (2016) 2115–2126, https://doi.org/10.1021/acs.accounts.6b00292.
[10] D.M. Charron, G. Zheng, Nanomedicine development guided by FRET imaging, Nano Today 18 (2018) 124–136, https://doi.org/10.1016/j.nantod.2017.12.006.
[11] B.M. Luby, D.M. Charron, C.M. MacLaughlin, G. Zheng, Activatable fluorescence: from small molecule to nanoparticle, Adv. Drug Deliv. Rev. 113 (2017) 97–121, https://doi.org/10.1016/j.addr.2016.08.010.
[12] R.T. Rebbeck, D.P. Singh, K.A. Janicek, D.M. Bers, D.D. Thomas, B.S. Launikonis, R.L. Cornea, RyR1-targeted drug discovery pipeline integrating FRET-based high-throughput screening and human myofiber dynamic Ca2+ assays, Sci. Rep. (2020), https://doi.org/10.1038/s41598-020-58461-1.
[13] J. Yoo, J.Y. Kim, J.M. Louis, I.V. Gopich, H.S. Chung, Fast three-color single-molecule FRET using statistical inference, Nat. Commun. (2020), https://doi.org/10.1038/s41467-020-17149-w.
[14] Y. Zhang, B. Ren, D. Zhang, Y. Liu, M. Zhang, C. Zhao, J. Zheng, Design principles and fundamental understanding of biosensors for amyloid-β detection, J. Mater. Chem. B (2020), https://doi.org/10.1039/d0tb00344a.
[15] A. Gansen, S. Felekyan, R. Kühnemuth, K. Lehmann, K. Tóth, C.A.M. Seidel, J. Langowski, High precision FRET studies reveal reversible transitions in nucleosomes between microseconds and minutes, Nat. Commun. (2018), https://doi.org/10.1038/s41467-018-06758-1.
[16] D. Nguyen, D.M. Behrens, S. Sen, A. Najdahmadi, J.N. Pham, G. Speciale, M. M. Lawrence, S. Majumdar, G.A. Weiss, E.L. Botvinick, Photostable and proteolysis-resistant förster resonance energy transfer-based calcium biosensor, Anal. Chem. (2020), https://doi.org/10.1021/acs.analchem.0c00573.
[17] J. Xu, J. Guo, N. Golob-Schwarzl, J. Haybaeck, X. Qiu, N. Hildebrandt, Single-Measurement multiplexed quantification of MicroRNAs from human tissue using catalytic hairpin assembly and förster resonance energy transfer, ACS Sens. (2020), https://doi.org/10.1021/acssensors.0c00432.
[18] J. Guo, C. Mingoes, X. Qiu, N. Hildebrandt, Simple, Ampli Fi Ed, and Multiplexed Detection of MicroRNAs Using Time-Gated FRET and Hybridization Chain Reaction, 2019, https://doi.org/10.1021/acs.analchem.8b05600.
[19] N. Zaman, K. Seitz, M. Kabir, L.S. George-Schreder, I. Shepstone, Y. Liu, S. Zhang, P.J. Krysan, A Förster resonance energy transfer sensor for live-cell imaging of mitogen-activated protein kinase activity in Arabidopsis, Plant J. (2019), https://doi.org/10.1111/tpj.14164.
[20] L. Wang, J. Wang, S. Xia, X. Wang, Y. Yu, H. Zhou, H. Liu, A FRET-based near-infrared ratiometric fluorescent probe for detection of mitochondria biothiol, Talanta 219 (2020) 121296, https://doi.org/10.1016/j.talanta.2020.121296.
[21] H. Jia, Y. Song, B. Huang, W. Ge, K.Q. Luo, Engineered sensor zebrafish for fast detection and real-time tracking of apoptosis at single-cell resolution in live animals, ACS Sens. (2020), https://doi.org/10.1021/acssensors.9b02489.
[22] K. Nie, B. Dong, H. Shi, L. Chao, M. Long, H. Xu, Z. Liu, B. Liang, Facile construction of AIE-based FRET nanoprobe for ratiometric imaging of hypochlorite in live cells, J. Lumin. 220 (2020) 117018, https://doi.org/10.1016/j.jlumin.2019.117018.
[23] X. Han, Z. Zhai, X. Yang, D. Zhang, J. Tang, J. Zhu, X. Zhu, Y. Ye, A FRET-based ratiometric fluorescent probe to detect cysteine metabolism in mitochondria, Org. Biomol. Chem. 18 (2020) 1487–1492, https://doi.org/10.1039/d0ob00002g.
[24] Q. Wan, T. Truongvo, H.E. Steele, A. Ozcelikkale, B. Han, Y. Wang, J. Oh, H. Yokota, S. Na, Subcellular domain-dependent molecular hierarchy of SFK and FAK in mechanotransduction and cytokine signaling, Sci. Rep. 7 (2017) 1–15, https://doi.org/10.1038/s41598-017-09495-5.
[25] J. Morla-Folch, G. Vargas-Nadal, T. Zhao, C. Sissa, A. Ardizzone, S. Kurhuzenkau, M. Köber, M. Uddin, A. Painelli, J. Veciana, K.D. Belfield, N. Ventosa, Dye-loaded quatsomes exhibiting FRET as nanoprobes for bioimaging, ACS Appl. Mater. Interfaces (2020), https://doi.org/10.1021/acsami.0c03040.
[26] T. Watabe, K. Terai, K. Sumiyama, M. Matsuda, Booster, a red-shifted genetically encoded förster resonance energy transfer (FRET) biosensor compatible with cyan fluorescent protein/yellow fluorescent protein-based FRET biosensors and blue light-responsive optogenetic tools, ACS Sens. 5 (2020) 719–730, https://doi.org/10.1021/acssensors.9b01941.
[27] Y. Konagaya, K. Terai, Y. Hirao, K. Takakura, M. Imajo, Y. Kamioka, N. Sasaoka, A. Kakizuka, K. Sumiyama, T. Asano, M. Matsuda, A highly sensitive FRET biosensor for AMPK exhibits heterogeneous AMPK responses among cells and organs, Cell Rep. 21 (2017) 2628–2638, https://doi.org/10.1016/j.celrep.2017.10.113.
[28] X. Zhou, Y. Liu, Q. Liu, L. Yan, M. Xue, W. Yuan, M. Shi, W. Feng, C. Xu, F. Li, Point-of-care ratiometric fluorescence imaging of tissue for the diagnosis of ovarian cancer, Theranostics 9 (2019) 4597–4607, https://doi.org/10.7150/thno.35322.
[29] N. Hildebrandt, C.M. Spillmann, W. Russ Algar, T. Pons, M.H. Stewart, E. Oh, K. Susumu, S.A. Díaz, J.B. Delehanty, I.L. Medintz, Energy transfer with semiconductor quantum dot bioconjugates: a versatile platform for biosensing, energy harvesting, and other developing applications, Chem. Rev. (2017), https://doi.org/10.1021/acs.chemrev.6b00030.
[30] M. Senarisoy, C. Barette, F. Lacroix, S. De Bonis, M. Stelter, F. Hans, J.P. Kleman, M.O. Fauvarque, J. Timmins, Förster resonance energy transfer based biosensor for targeting the hNTH1-YB1 interface as a potential anticancer drug target, ACS Chem. Biol. (2020), https://doi.org/10.1021/acschembio.9b01023.
[31] H. Schneider, L. Deweid, O. Avrutina, H. Kolmar, Recent progress in transglutaminase-mediated assembly of antibody-drug conjugates, Anal. Biochem. (2020), https://doi.org/10.1016/j.ab.2020.113615.
[32] S.A. Hussain, S. Chakraborty, Organoclay Hybrid Films with Improved Functionality, Elsevier Inc., 2017, https://doi.org/10.1016/B978-0-323-46153-5.00008-2.
[33] S. Chen, Y.L. Yu, Fluorescence resonance energy transfer (FRET) spectroscopy, Encycl. Anal. Sci. (2019), https://doi.org/10.1016/B978-0-12-409547-2.13944-7.
[34] D. Hamers, L. van Voorst Vader, J.W. Borst, J. Goedhart, Development of FRET biosensors for mammalian and plant systems, Protoplasma (2014), https://doi.org/10.1007/s00709-013-0590-z.

[35] S.H. Park, W. Ko, H.S. Lee, I. Shin, Analysis of protein-protein interaction in a single live cell by using a FRET system based on genetic code expansion technology, J. Am. Chem. Soc. (2019), https://doi.org/10.1021/jacs.8b10098.
[36] K.T. Kim, Y. Moon, Y. Jang, K.T. Lee, C. Lee, Y. Jun, S. Lee, Molecular mechanisms of atlastin-mediated ER membrane fusion revealed by a FRET-based single-vesicle fusion assay, Sci. Rep. (2017), https://doi.org/10.1038/s41598-017-09162-9.
[37] A.D. Roy, J. Saha, D. Dey, D. Bhattacharjee, S.A. Hussain, Investigation on ionic states of 1,2-Dipalmitoyl-sn-glycero-3-phosphorylcholine (DPPC) using organic laser dyes: a FRET study, J. Lumin. (2017), https://doi.org/10.1016/j.jlumin.2016.12.040.
[38] H. Zhou, G. Tourkakis, D. Shi, D.M. Kim, H. Zhang, T. Du, W.C. Eades, M. Y. Berezin, Cell-free measurements of brightness of fluorescently labeled antibodies, Sci. Rep. 7 (2017) 1–9, https://doi.org/10.1038/srep41819.
[39] T. Thomsen, A.B. Ayoub, D. Psaltis, H.A. Klok, Fluorescence-based and fluorescent label-free characterization of polymer nanoparticle decorated T cells, Biomacromolecules 22 (2021) 190–200, https://doi.org/10.1021/acs.biomac.0c00969.
[40] J.F. Joung, M. Han, M. Jeong, S. Park, Experimental database of optical properties of organic compounds, Sci. Data. 7 (2020) 1–7, https://doi.org/10.1038/s41597-020-00634-8.
[41] J. Shi, F. Tian, J. Lyu, M. Yang, Nanoparticle based fluorescence resonance energy transfer (FRET) for biosensing applications, J. Mater. Chem. B. 3 (2015) 6989–7005, https://doi.org/10.1039/c5tb00885a.
[42] Y. Gawale, N. Sekar, Investigating the excited state optical properties and origin of large Stokes shift in Benz[c,d]indole N-Heteroarene BF2 dyes with ab initio tools, J. Photochem. Photobiol. B Biol. 178 (2018) 472–480, https://doi.org/10.1016/j.jphotobiol.2017.12.006.
[43] Z. Gao, Y. Hao, M. Zheng, Y. Chen, A fluorescent dye with large Stokes shift and high stability: synthesis and application to live cell imaging, RSC Adv. 7 (2017) 7604–7609, https://doi.org/10.1039/c6ra27547h.
[44] X.X. Zhang, Z. Wang, X. Yue, Y. Ma, D.O. Kiesewetter, X. Chen, PH-sensitive fluorescent dyes: are they really ph-sensitive in cells? Mol. Pharm. 10 (2013) 1910–1917, https://doi.org/10.1021/mp3006903.
[45] D. Broadwater, M. Bates, M. Jayaram, M. Young, J. He, A.L. Raithel, T. W. Hamann, W. Zhang, B. Borhan, R.R. Lunt, S.Y. Lunt, Modulating cellular cytotoxicity and phototoxicity of fluorescent organic salts through counterion pairing, Sci. Rep. 9 (2019) 1–11, https://doi.org/10.1038/s41598-019-51593-z.
[46] D. Wüstner, T. Christensen, L.M. Solanko, D. Sage, Photobleaching kinetics and time-integrated emission of fluorescent probes in cellular membranes, Molecules 19 (2014) 11096–11130, https://doi.org/10.3390/molecules190811096.
[47] Y. Shen, S.Y. Wu, V. Rancic, A. Aggarwal, Y. Qian, S.I. Miyashita, K. Ballanyi, R. E. Campbell, M. Dong, Genetically encoded fluorescent indicators for imaging intracellular potassium ion concentration, Commun. Biol. (2019), https://doi.org/10.1038/s42003-018-0269-2.
[48] M. Mastop, D.S. Bindels, N.C. Shaner, M. Postma, T.W.J. Gadella, J. Goedhart, Characterization of a spectrally diverse set of fluorescent proteins as FRET acceptors for mTurquoise2, Sci. Rep. (2017), https://doi.org/10.1038/s41598-017-12212-x.
[49] F. Cardarelli, Back to the future: genetically encoded fluorescent proteins as inert tracers of the intracellular environment, Int. J. Mol. Sci. 21 (2020) 1–17, https://doi.org/10.3390/ijms21114164.
[50] P.J. Cranfill, B.R. Sell, M.A. Baird, J.R. Allen, Z. Lavagnino, H.M. De Gruiter, G. J. Kremers, M.W. Davidson, A. Ustione, D.W. Piston, Quantitative assessment of fluorescent proteins, Nat. Methods 13 (2016) 557–562, https://doi.org/10.1038/nmeth.3891.
[51] M.G. Romei, S.G. Boxer, Split GFP: scope, limitations and outlook, Annu. Rev. Biophys. 176 (2019) 139–148, https://doi.org/10.1146/annurev-biophys-051013-022846.Split.
[52] R. Wang, S. Xiang, Y. Zhang, Q. Chen, Y. Zhong, S. Wang, Development of a functional antibody by using a green fluorescent protein frame as the template, Appl. Environ. Microbiol. 80 (2014) 4126–4137, https://doi.org/10.1128/AEM.00936-14.
[53] A. Chandra, S. Prasad, G. Gigli, L.L. del Mercato, Fluorescent nanoparticles for sensing, Front. Nanosci. 16 (2020) 117–149, https://doi.org/10.1016/B978-0-08-102828-5.00006-1.
[54] S.H. Qaddare, A. Salimi, Amplified fluorescent sensing of DNA using luminescent carbon dots and AuNPs/GO as a sensing platform: a novel coupling of FRET and DNA hybridization for homogeneous HIV-1 gene detection at femtomolar level, Biosens. Bioelectron. 89 (2017) 773–780, https://doi.org/10.1016/j.bios.2016.10.033.
[55] Z. Heger, N. Cernei, S. Krizkova, M. Masarik, P. Kopel, P. Hodek, O. Zitka, V. Adam, R. Kizek, Paramagnetic nanoparticles as a platform for FRET-based sarcosine picomolar detection, Sci. Rep. (2015), https://doi.org/10.1038/srep08868.
[56] N. Melnychuk, A.S. Klymchenko, DNA-functionalized dye-loaded polymeric nanoparticles: ultrabright FRET platform for amplified detection of nucleic acids, J. Am. Chem. Soc. (2018), https://doi.org/10.1021/jacs.8b05840.
[57] F. Radnia, N. Mohajeri, N. Zarghami, New Insight into the Engineering of Green Carbon Dots: Possible Applications in Emerging Cancer Theranostics, Talanta, 2020, https://doi.org/10.1016/j.talanta.2019.120547.
[58] B. Zhou, Y.T. Chen, X.L. Zhen, L. Lou, Yong-Sheng Wang, Q.L. Suo, Fluorescent resonance energy transfer of organic fluorescent dyes with gold nanoparticles and their analytical application, Gold Bull. (2018), https://doi.org/10.1007/s13404-018-0240-5.
[59] X. Liu, Y. Hou, S. Chen, J. Liu, Controlling dopamine binding by the new aptamer for a FRET-based biosensor, Biosens. Bioelectron. (2021), https://doi.org/10.1016/j.bios.2020.112798.
[60] W. Dong, R. Wang, X. Gong, C. Dong, An efficient turn-on fluorescence biosensor for the detection of glutathione based on FRET between N,S dual-doped carbon dots and gold nanoparticles, Anal. Bioanal. Chem. (2019), https://doi.org/10.1007/s00216-019-02042-3.
[61] X. Qiu, J. Guo, J. Xu, N. Hildebrandt, Three-dimensional FRET multiplexing for DNA quantification with attomolar detection limits, J. Phys. Chem. Lett. (2018), https://doi.org/10.1021/acs.jpclett.8b01944.
[62] N. Melnychuk, S. Egloff, A. Runser, A. Reisch, A.S. Klymchenko, Light-Harvesting nanoparticle probes for FRET-based detection of oligonucleotides with single-molecule sensitivity, Angew. Chem. Int. Ed. (2020), https://doi.org/10.1002/anie.201913804.
[63] A. Afzalinia, M. Mirzaee, Ultrasensitive Fluorescent miRNA Biosensor Based on a " Sandwich " Oligonucleotide Hybridization and Fluorescence Resonance Energy Transfer Process Using an Ln(III)-MOF and Ag Nanoparticles for Early Cancer Diagnosis: Application of Central Composite Desi, 2020, https://doi.org/10.1021/acsami.0c00891.
[64] S. Deng, J. Wu, K. Zhang, Y. Li, L. Yang, D. Hu, Y. Jin, Y. Hao, X. Wang, Y. Liu, H. Liu, Y. Chen, M. Xie, Fluorescence resonance energy transfer-mediated immunosensor based on design and synthesis of the substrate of amp cephalosporinase for biosensing, Anal. Chem. 3 (2019) 11316–11323, https://doi.org/10.1021/acs.analchem.9b02427.
[65] T. Kondo, M. Fujioka, S. Fujisawa, K. Sato, M. Tsuda, T. Miyagishima, A. Mori, H. Iwasaki, Y. Kakinoki, S. Yamamoto, Y. Haseyama, S. Ando, M. Shindo, S. Ota, M. Kurosawa, Y. Ohba, T. Teshima, Clinical efficacy and safety of first-line nilotinib therapy and evaluation of the clinical utility of the FRET-based drug sensitivity test, Int. J. Hematol. (2019), https://doi.org/10.1007/s12185-019-02696-w.
[66] A. Shteinfer-Kuzmine, A. Verma, T. Arif, O. Aizenberg, A. Paul, V. Shoshan-Barmaz, Mitochondria and nucleus cross-talk: signaling in metabolism, apoptosis, and differentiation, and function in cancer, IUBMB Life 73 (2021) 492–510, https://doi.org/10.1002/iub.2407.
[67] S. Mehta, Y. Zhang, R.H. Roth, J. fan Zhang, A. Mo, B. Tenner, R.L. Huganir, J. Zhang, Single-fluorophore biosensors for sensitive and multiplexed detection of signalling activities, Nat. Cell Biol. (2018), https://doi.org/10.1038/s41556-018-0200-6.
[68] F. Grisan, M. Spacci, C. Paoli, A. Costamagna, M. Fantuz, M. Martini, K. Lefkimmiatis, A. Carrer, Cholesterol activates cyclic AMP signaling in metaplastic acinar cells, Metabolites 11 (2021) 141, https://doi.org/10.3390/metabo11030141.
[69] B.W. Davis, N. Niamnont, R. Dillon, C.J. Bardeen, M. Sukwattanasinitt, Q. Cheng, FRET detection of proteins using fluorescently doped electrospun nanofibers and pattern recognition, Langmuir 27 (2011) 6401–6408, https://doi.org/10.1021/la2006925.
[70] J. Zhang, W. qing Qiu, H. Zhu, H. Liu, J. hua Sun, Y. Chen, H. Shen, C. lin Qian, Z. yong Shen, HOTAIR contributes to the carcinogenesis of gastric cancer via modulating cellular and exosomal miRNAs level, Cell Death Dis. 11 (2020), https://doi.org/10.1038/s41419-020-02946-4.
[71] L. Liu, Q. Rong, G. Ke, M. Zhang, J. Li, Y. Li, Y. Liu, M. Chen, X.B. Zhang, Efficient and reliable MicroRNA imaging in living cells via a FRET-based localized hairpin-DNA cascade amplifier, Anal. Chem. (2019), https://doi.org/10.1021/acs.analchem.8b05778.
[72] H. Zhao, M. Wang, X. Xiong, Y. Liu, X. Chen, Simultaneous fluorescent detection of multiplexed miRNA of liver cancer based on DNA tetrahedron nanotags, Talanta 210 (2020) 120677, https://doi.org/10.1016/j.talanta.2019.120677.
[73] Y.S. Borghei, M. Hosseini, M.R. Ganjali, Fluorometric determination of microRNA via FRET between silver nanoclusters and CdTe quantum dots, Microchim. Acta. 184 (2017) 4713–4721, https://doi.org/10.1007/s00604-017-2512-9.
[74] H. Tian, C. Yuan, Y. Liu, Z. Li, K. Xia, M. Li, F. Xie, Q. Chen, M. Chen, W. Fu, Y. Zhang, A novel quantification platform for point-of-care testing of circulating MicroRNAs based on allosteric spherical nanoprobe, J. Nanobiotechnol. 18 (2020) 1–11, https://doi.org/10.1186/s12951-020-00717-z.
[75] A. Manuscript, rsc.li/analyst (2020), https://doi.org/10.1039/C9AN02610J.
[76] F.R. Nitu, L. Savu, S. Muraru, I. Stoian, M. Ionită, Label-free homogeneous microRNA detection in cell culture medium based on graphene oxide and specific fluorescence quenching, Nanomaterials 11 (2021) 1–11, https://doi.org/10.3390/nano11020368.
[77] A. Manuscript, Mater. Chem. B (2017), https://doi.org/10.1039/C7TB01399J.
[78] J. Xu, J. Guo, N. Golob-schwarzl, J. Haybaeck, X. Qiu, N. Hildebrandt, Single-measurement multiplexed quantification of microRNAs from human tissue using catalytic hairpin assembly and Förster resonance energy transfer Single-measurement multiplexed quantification of microRNAs from human tissue using catalytic hairpin assemb, ACS Sens. 5 (2020) 1768–1776, https://doi.org/10.1021/acssensors.0c00432.
[79] B. Wang, Z. You, D. Ren, Target-assisted FRET signal amplification for ultrasensitive detection of microRNA, Analyst 144 (2019) 2304–2311, https://doi.org/10.1039/c8an02266f.
[80] L. He, D.Q. Lu, H. Liang, S. Xie, C. Luo, M. Hu, L. Xu, X. Zhang, W. Tan, Fluorescence resonance energy transfer-based DNA tetrahedron nanotweezer for highly reliable detection of tumor-related mRNA in living cells, ACS Nano (2017), https://doi.org/10.1021/acsnano.7b00725.
[81] G. Bertolin, F. Sizaire, G. Herbomel, D. Reboutier, C. Prigent, M. Tramier, A FRET biosensor reveals spatiotemporal activation and functions of aurora kinase A in

living cells, Nat. Commun. 7 (2016) 1–16, https://doi.org/10.1038/ncomms12674.
[82] D.M. Yang, T.F. Fu, C.S. Lin, T.Y. Chiu, C.C. Huang, H.Y. Huang, M.W. Chung, Y. S. Lin, R.V. Manurung, P.N.N. Nguyen, Y.F. Chang, High-performance FRET biosensors for single-cell and in vivo lead detection, Biosens. Bioelectron. (2020), https://doi.org/10.1016/j.bios.2020.112571.
[83] A. Das, T. Dutta, L. Gadhe, A.L. Koner, I. Saraogi, Biocompatible fluorescent probe for selective detection of amyloid fibrils, Anal. Chem. (2020), https://doi.org/10.1021/acs.analchem.0c00379.
[84] L. Sewell, F. Stylianou, Y. Xu, J. Taylor, L. Sefer, S. Matthews, NMR insights into the pre-amyloid ensemble and secretion targeting of the curli subunit CsgA, Sci. Rep. (2020), https://doi.org/10.1038/s41598-020-64135-9.
[85] N. Ojha, K.H. Rainey, G.H. Patterson, Imaging of fluorescence anisotropy during photoswitching provides a simple readout for protein self-association, Nat. Commun. (2020), https://doi.org/10.1038/s41467-019-13843-6.
[86] S.T. Sowa, C. Vela-Rodríguez, A. Galera-Prat, M. Cázares-Olivera, R. Prunskaite-Hyyryläinen, A. Ignatev, L. Lehtiö, A FRET-based high-throughput screening platform for the discovery of chemical probes targeting the scaffolding functions of human tankyrases, Sci. Rep. (2020), https://doi.org/10.1038/s41598-020-69229-y.
[87] S. Karmakar, S.K. Mukherjee, H. Lal, S. Biswas, P.P. Jani, P.K. Chowdhury, Crowder induced structural modulation of a multi-domain protein during its early stages of aggregation: a FRET-based and protein solvation study, Int. J. Biol. Macromol. (2019), https://doi.org/10.1016/j.ijbiomac.2019.01.054.
[88] C.H. Lo, N.K. Pandey, C.K.-W. Lim, Z. Ding, M. Tao, D.D. Thomas, R. Langen, J. N. Sachs, Discovery of small molecule inhibitors of huntingtin exon 1 aggregation by FRET-based high-throughput screening in living cells, ACS Chem. Neurosci. (2020), https://doi.org/10.1021/acschemneuro.0c00226.
[89] D.M. Shcherbakova, N. Cox Cammer, T.M. Huisman, V.V. Verkhusha, L. Hodgson, Direct multiplex imaging and optogenetics of Rho GTPases enabled by near-infrared FRET article, Nat. Chem. Biol. (2018), https://doi.org/10.1038/s41589-018-0044-1.
[90] N. Soleja, O. Manzoor, P. Nandal, M. Mohsin, FRET-based nanosensors for monitoring and quantification of alcohols in living cells, Org, Biomol. Chem. (2019), https://doi.org/10.1039/c8ob03208d.
[91] M. Borecki, M.L. Korwin-Pawlowski, Optical capillary sensors for intelligent microfluidic sample classification, Nanosensors Theory Appl. Ind. Heal. Def. (2011).
[92] W. Wang, N. Li, J.T. Liu, J.Y. Miao, B.X. Zhao, Z.M. Lin, A new FRET-based ratiometric fluorescent probe for the detection of SO2 derivatives in mitochondria of living cells, Dye, Pigment 181 (2020), https://doi.org/10.1016/j.dyepig.2020.108639.
[93] A. Manuscript, Biomolecular Chemistry (2020), https://doi.org/10.1039/D0OB00002G.
[94] X. Ji, S. Xie, Y. Jiao, X. Zhang, D. Sun, V.C. Yang, M. Wang, H. He, L. Sun, MT1-MMP activatable fluorogenic probes with enhanced specificity: via high-affinity peptide conjugation for tumor imaging, Biomater. Sci. 8 (2020) 2308–2317, https://doi.org/10.1039/c9bm02007a.
[95] P. Sontisiri, P. Yingyuad, P. Thongyoo, A highly selective “Turn On” fluorescent probe based on FRET mechanism for hydrogen sulfide detection in living cells, J. Photochem. Photobiol. Chem. 391 (2020) 112401, https://doi.org/10.1016/j.jphotochem.2020.112401.
[96] S. Bernegger, C. Brunner, M. Vizovišek, M. Fonovic, G. Cuciniello, F. Giordano, V. Stanojlovic, M. Jarzab, P. Simister, S.M. Feller, G. Obermeyer, G. Posselt, B. Turk, C. Cabrele, G. Schneider, S. Wessler, A novel FRET peptide assay reveals efficient Helicobacter pylori HtrA inhibition through zinc and copper binding, Sci. Rep. (2020), https://doi.org/10.1038/s41598-020-67578-2.
[97] X. Bi, J. Yin, D. Zhang, X. Zhang, S. Balamkundu, J. Lescar, P.C. Dedon, J.P. Tam, C.-F. Liu, Tagging transferrin receptor with a disulfide FRET probe to gauge the redox state in endosomal compartments, Anal. Chem. (2020), https://doi.org/10.1021/acs.analchem.0c02264.
[98] A. Bigdeli, F. Ghasemi, S. Abbasi-Moayed, M. Shahrajabian, N. Fahimi-Kashani, S. Jafarinejad, M.A. Farahmand Nejad, M.R. Hormozi-Nezhad, Ratiometric fluorescent nanoprobes for visual detection: design principles and recent advances - a review, Anal. Chim. Acta 1079 (2019) 30–58, https://doi.org/10.1016/j.aca.2019.06.035.
[99] L. Liu, H. Zhang, Z. Wang, D. Song, Peptide-functionalized upconversion nanoparticles-based FRET sensing platform for Caspase-9 activity detection in vitro and in vivo, Biosens. Bioelectron. 141 (2019) 111403, https://doi.org/10.1016/j.bios.2019.111403.
[100] S.G. Sun, H. Ding, G. Yuan, L. Zhou, An efficient TP-FRET-based lysosome-targetable fluorescent probe for imaging peroxynitrite with two well-resolved emission channels in living cells, tissues and zebrafish, Anal. Chim. Acta 1100 (2020) 200–207, https://doi.org/10.1016/j.aca.2019.11.065.
[101] S. Ghosh, Y.F. Chang, D.M. Yang, S. Chattopadhyay, Upconversion nanoparticle-mOrange protein FRET nanoprobes for self-ratiometric/ratiometric determination of intracellular pH, and single cell pH imaging, Biosens. Bioelectron. 155 (2020) 112115, https://doi.org/10.1016/j.bios.2020.112115.
[102] B. Dong, M. Tian, X. Kong, W. Song, Y. Lu, W. Lin, Förster resonance energy transfer-based fluorescent probe for the selective imaging of hydroxylamine in living cells, Anal. Chem. 91 (2019) 11397–11402, https://doi.org/10.1021/acs.analchem.9b02737.
[103] Z. Zhang, Q. Feng, M. Yang, Y. Tang, A ratiometric fluorescent biosensor based on conjugated polymers for sensitive detection of nitroreductase and hypoxia diagnosis in tumor cells, Sensor. Actuator. B Chem. 318 (2020) 128257, https://doi.org/10.1016/j.snb.2020.128257.
[104] J. He, S. Wink, H. de Bont, S. Le Dévédec, Y. Zhang, B. van de Water, FRET biosensor-based kinase inhibitor screen for ERK and AKT activity reveals differential kinase dependencies for proliferation in TNBC cells, Biochem. Pharmacol. 169 (2019) 113640, https://doi.org/10.1016/j.bcp.2019.113640.
[105] T. Deng, X. Wang, S. Wu, S. Hu, W. Liu, T. Chen, Z. Yu, Q. Xu, F. Liu, A new FRET probe for ratiometric fluorescence detecting mitochondria-localized drug activation and imaging endogenous hydroxyl radicals in zebrafish, Chem. Commun. 56 (2020) 4432–4435, https://doi.org/10.1039/d0cc00382d.
[106] R.T.K. Kwok, C.W.T. Leung, J.W.Y. Lam, B.Z. Tang, Biosensing by luminogens with aggregation-induced emission characteristics, Chem. Soc. Rev. (2015), https://doi.org/10.1039/c4cs00325j.
[107] X. He, F. Ding, W. Xu, C. Xu, Y. Li, Y. Qian, S. Zhao, H. Chen, J. Shen, FRET-based colorimetric and ratiometric sensor for visualizing pH change and application for bioimaging in living cells, bacteria and zebrafish, Anal. Chim. Acta 1127 (2020) 29–38, https://doi.org/10.1016/j.aca.2020.06.031.
[108] Y. Kamioka, K. Sumiyama, R. Mizuno, Y. Sakai, E. Hirata, E. Kiyokawa, M. Matsuda, Live imaging of protein kinase activities in transgenic mice expressing FRET biosensors, Cell Struct. Funct. 37 (2012) 65–73, https://doi.org/10.1247/csf.11045.
[109] M. Jing, P. Zhang, G. Wang, J. Feng, L. Mesik, J. Zeng, H. Jiang, S. Wang, J. C. Looby, N.A. Guagliardo, L.W. Langma, J. Lu, Y. Zuo, D.A. Talmage, L.W. Role, P.Q. Barrett, L.I. Zhang, M. Luo, Y. Song, J.J. Zhu, Y. Li, A genetically encoded fluorescent acetylcholine indicator for in vitro and in vivo studies, Nat. Biotechnol. 36 (2018), https://doi.org/10.1038/nbt.4184.
[110] H. Bischof, M. Rehberg, S. Stryeck, K. Artinger, E. Eroglu, M. Waldeck-Weiermair, B. Gottschalk, R. Rost, A.T. Deak, T. Niedrist, N. Vujic, H. Lindermuth, R. Prassl, B. Pelzmann, K. Groschner, D. Kratky, K. Eller, A.R. Rosenkranz, T. Madl, N. Plesnila, W.F. Graier, R. Malli, Novel genetically encoded fluorescent probes enable real-Time detection of potassium in vitro and in vivo, Nat. Commun. 8 (2017) 1–11, https://doi.org/10.1038/s41467-017-01615-z.
[111] C.M. Díaz-García, C. Lahmann, J.R. Martínez-François, B. Li, D. Koveal, N. Nathwani, M. Rahman, J.P. Keller, J.S. Marvin, L.L. Looger, G. Yellen, Quantitative in vivo imaging of neuronal glucose concentrations with a genetically encoded fluorescence lifetime sensor, J. Neurosci. Res. 97 (2019) 946–960, https://doi.org/10.1002/jnr.24433.
[112] A. Duro-Castano, N.H. Lim, I. Tranchant, M. Amoura, F. Beau, H. Wieland, O. Kingler, M. Herrmann, M. Nazaré, O. Plettenburg, V. Dive, M.J. Vicent, H. Nagase, Vivo imaging of MMP-13 activity using a specific polymer-FRET peptide conjugate detects early osteoarthritis and inhibitor efficacy, Adv. Funct. Mater. 28 (2018) 1–9, https://doi.org/10.1002/adfm.201802738.
[113] F. Cayre, S. Mura, B. Andreiuk, D. Sobot, S. Gouazou, D. Desmaële, A. S. Klymchenko, P. Couvreur, Vivo FRET imaging to predict the risk associated with hepatic accumulation of squalene-based prodrug nanoparticles, Adv. Healthc. Mater. 7 (2018) 1–7, https://doi.org/10.1002/adhm.201700830.
[114] A.A. Shemetov, M.V. Monakhov, Q. Zhang, J.E. Canton-Josh, M. Kumar, M. Chen, M.E. Matlashov, X. Li, W. Yang, L. Nie, D.M. Shcherbakova, Y. Kozorovitskiy, J. Yao, N. Ji, V.V. Verkhusha, A near-infrared genetically encoded calcium indicator for in vivo imaging, Nat. Biotechnol. 39 (2021) 368–377, https://doi.org/10.1038/s41587-020-0710-1.
[115] M. Nobis, D. Herrmann, S.C. Warren, S. Kadir, W. Leung, M. Killen, A. Magenau, D. Stevenson, M.C. Lucas, N. Reischmann, C. Vennin, J.R.W. Conway, A. Boulghourjian, A. Zaratzian, A.M. Law, D. Gallego-Ortega, C.J. Ormandy, S. N. Walters, S.T. Grey, J. Bailey, T. Chtanova, J.M.W. Quinn, P.A. Baldock, P. I. Croucher, J.P. Schwarz, A. Mrowinska, L. Zhang, H. Herzog, A. Masedunskas, E. C. Hardeman, P.W. Gunning, G. del Monte-Nieto, R.P. Harvey, M.S. Samuel, M. Pajic, E.J. McGhee, A.K.E. Johnsson, O.J. Sansom, H.C.E. Welch, J.P. Morton, D. Strathdee, K.I. Anderson, P. Timpson, A RhoA-FRET biosensor mouse for intravital imaging in normal tissue homeostasis and disease contexts, Cell Rep. 21 (2017) 274–288, https://doi.org/10.1016/j.celrep.2017.09.022.
[116] M. Ahmad, N.A. Anjum, A. Asif, A. Ahmad, Real-time monitoring of glutathione in living cells using genetically encoded FRET-based ratiometric nanosensor, Sci. Rep. 10 (2020) 1–9, https://doi.org/10.1038/s41598-020-57654-y.
[117] S. Yoshikawa, T. Usami, J. Kikuta, M. Ishii, T. Sasano, K. Sugiyama, T. Furukawa, E. Nakasho, H. Takayanagi, T.F. Tedder, H. Karasuyama, A. Miyawaki, T. Adachi, Intravital imaging of Ca2+ signals in lymphocytes of Ca2+ biosensor transgenic mice: indication of autoimmune diseases before the pathological onset, Sci. Rep. 6 (2016) 1–13, https://doi.org/10.1038/srep18738.
[118] D.M. Yang, R.V. Manurung, Y.S. Lin, T.Y. Chiu, W.Q. Lai, Y.F. Chang, T.F. Fu, Monitoring the heavy metal lead inside living drosophila with a FRET-based biosensor, Sensors 20 (2020) 1–14, https://doi.org/10.3390/s20061712.
[119] S. Schobesberger, P.T. Wright, C. Poulet, J.L. Sanchez-Alonso, C. Mansfield, A. Friebe, S.E. Harding, J.L. Balligand, V.O. Nikolaev, J. Gorelik, β-Adrenoceptor Redistribution Impairs NO/cGMP/PDE2 Signalling in 4 Failing Cardiomyocytes, Elife, 2020, https://doi.org/10.7554/eLife.52221.
[120] G. Rong, S.R. Corrie, H.A. Clark, Vivo biosensing: progress and perspectives, ACS Sens. 2 (2017) 327–338, https://doi.org/10.1021/acssensors.6b00834.
[121] Z. Tang, X. Liu, B. Su, Q. Chen, H. Cao, Y. Yun, Y. Xu, B.D. Hammock, Ultrasensitive and rapid detection of ochratoxin A in agro-products by a nanobody-mediated FRET-based immunosensor, J. Hazard Mater. (2020), https://doi.org/10.1016/j.jhazmat.2019.121678.
[122] W. Yang, Y. Shen, D. Zhang, W. Xu, Protein-responsive rolling circle amplification as a tandem template to drive amplified transduction of fluorescence signal probes for highly sensitive immunoassay, Chem. Commun. (2018), https://doi.org/10.1039/C8CC04395G.
[123] N. Mohajeri, E. Mostafavi, N. Zarghami, The feasibility and usability of DNA-dot bioconjugation to antibody for targeted in vitro cancer cell fluorescence imaging,

J. Photochem. Photobiol. B Biol. (2020), https://doi.org/10.1016/j.jphotobiol.2020.111944.
[124] S. Mohammadi, A. Salimi, S. Hamd-Ghadareh, F. Fathi, F. Soleimani, A FRET immunosensor for sensitive detection of CA 15-3 tumor marker in human serum sample and breast cancer cells using antibody functionalized luminescent carbon-dots and AuNPs-dendrimer aptamer as donor-acceptor pair, Anal. Biochem. (2018), https://doi.org/10.1016/j.ab.2018.06.008.
[125] S. Bagdeli, A.H. Rezayan, R.A. Taheri, M. Kamali, M. Hosseini, FRET- based immunoassay using CdTe and AuNPs for the detection of OmpW antigen of Vibrio cholerae, J. Lumin. 192 (2017) 932–939, https://doi.org/10.1016/j.jlumin.2017.08.032.
[126] Z. Dehghani, J. Mohammadnejad, M. Hosseini, B. Bakhshi, A.H. Rezayan, Whole cell FRET immunosensor based on graphene oxide and graphene dot for Campylobacter jejuni detection, Food Chem. (2020), https://doi.org/10.1016/j.foodchem.2019.125690.
[127] B. Heli, A. Ajji, Toward a nanopaper-based and solid phase immunoassay using FRET for the rapid detection of bacteria, Sci. Rep. 10 (2020) 1–11, https://doi.org/10.1038/s41598-020-71285-3.
[128] Y. Nie, J. Li, Y. Liu, Q. Zhang, Q. Ma, A visual FRET immunofluorescent biosensor for ratiometric parathyroid hormone (1–84) antigen point-of-care detection, J. Fluoresc. (2020), https://doi.org/10.1007/s10895-020-02502-5.
[129] O.A. Goryacheva, N.V. Beloglazova, I.Y. Goryacheva, S. De Saeger, Homogenous FRET-based fluorescent immunoassay for deoxynivalenol detection by controlling the distance of donor-acceptor couple, Talanta 225 (2021) 121973, https://doi.org/10.1016/j.talanta.2020.121973.
[130] X. Weng, S. Neethirajan, Immunosensor based on antibody-functionalized MoS2 for rapid detection of avian coronavirus on cotton thread, IEEE Sensor. J. (2018), https://doi.org/10.1109/JSEN.2018.2829084.
[131] S. Gogoi, R. Khan, Fluorescence immunosensor for cardiac troponin T based on Förster resonance energy transfer (FRET) between carbon dot and MoS2 nano-couple, Phys. Chem. Chem. Phys. 20 (2018) 16501–16509, https://doi.org/10.1039/c8cp02433b.
[132] L. Miao, C. Zhu, L. Jiao, H. Li, D. Du, Y. Lin, Q. Wei, Smart drug delivery system-inspired enzyme-linked immunosorbent assay based on fluorescence resonance energy transfer and allochroic effect induced dual-modal colorimetric and fluorescent detection, Anal. Chem. (2018), https://doi.org/10.1021/acs.analchem.7b04068.
[133] F. Weihs, A. Anderson, S. Trowell, K. Caron, Resonance energy transfer-based biosensors for point-of-need diagnosis—progress and perspectives, Sensors 21 (2021) 1–18, https://doi.org/10.3390/s21020660.
[134] S. Sakamoto, W. Putalun, S. Vimolmangkang, W. Phoolcharoen, Y. Shoyama, H. Tanaka, S. Morimoto, Enzyme-linked immunosorbent assay for the quantitative/qualitative analysis of plant secondary metabolites, J. Nat. Med. 72 (2018) 32–42, https://doi.org/10.1007/s11418-017-1144-z.
[135] L. Zhou, F. Ji, T. Zhang, F. Wang, Y. Li, Z. Yu, X. Jin, B. Ruan, An fluorescent aptasensor for sensitive detection of tumor marker based on the FRET of a sandwich structured QDs-AFP-AuNPs, Talanta 197 (2019) 444–450, https://doi.org/10.1016/j.talanta.2019.01.012.
[136] P. Gong, L. Zhang, J. Peng, S. Li, J. Chen, X. Liu, H. Peng, Z. Liu, J. You, Smart "on-off-on" fluorescent switches for drug visual loading and responsive delivery, Dyes Pigments 173 (2020) 107893, https://doi.org/10.1016/j.dyepig.2019.107893.
[137] Z. Dong, Y. Bi, H. Cui, Y. Wang, C. Wang, Y. Li, H. Jin, C. Wang, AIE supramolecular assembly with FRET effect for visualizing drug delivery, ACS Appl. Mater. Interfaces (2019), https://doi.org/10.1021/acsami.9b04938.
[138] F. Taemaitree, B. Fortuni, Y. Koseki, E. Fron, S. Rocha, J. Hofkens, H. Uji-i, T. Inose, H. Kasai, FRET-based intracellular investigation of nanoprodrugs toward highly efficient anticancer drug delivery, Nanoscale 12 (2020) 16710–16715, https://doi.org/10.1039/d0nr04910g.
[139] Y. Fu, X. Chen, X. Mou, Z. Ren, X. Li, G. Han, A dual-color luminescent localized drug delivery system with ratiometric-monitored doxorubicin release functionalities, ACS Biomater. Sci. Eng. (2016), https://doi.org/10.1021/acsbiomaterials.6b00046.
[140] L.I. Selby, L. Aurelio, D. Yuen, B. Graham, A.P.R. Johnston, Quantifying cellular internalization with a fluorescent click sensor, ACS Sens. (2018), https://doi.org/10.1021/acssensors.8b00219.
[141] C. Du, Y. Liang, Q. Ma, Q. Sun, J. Qi, J. Cao, S. Han, M. Liang, B. Song, Y. Sun, Intracellular tracking of drug release from pH-sensitive polymeric nanoparticles via FRET for synergistic chemo-photodynamic therapy, J. Nanobiotechnol. (2019), https://doi.org/10.1186/s12951-019-0547-2.
[142] S. Scarabelli, K.T. Tan, R. Griss, R. Hovius, P.L. D'Alessandro, T. Vorherr, K. Johnsson, Evaluating cellular drug uptake with fluorescent sensor proteins, ACS Sens. (2017), https://doi.org/10.1021/acssensors.7b00331.
[143] B.C. Lee, C. Chalouni, S. Doll, S.C. Nalle, M. Darwish, S.P. Tsai, K.R. Kozak, G. Del-Rosario, S.F. Yu, H. Erickson, R. Vandlen, FRET reagent reveals the intracellular processing of peptide-linked antibody-drug conjugates, Bioconjugate Chem. (2018), https://doi.org/10.1021/acs.bioconjchem.8b00362.
[144] H. Wang, D.L. Shi, J. Li, H.Y. Tang, J. Li, Y. Guo, A facile fluorescent probe with a large Stokes shift for sequentially detecting copper and sulfide in 100% aqueous solution and imaging them in living cells, Sensor. Actuator. B Chem. (2018), https://doi.org/10.1016/j.snb.2017.10.124.
[145] Y. Wen, S. Cahya, W. Zeng, J. Lin, X. Wang, L. Liu, L. Malherbe, R. Siegel, A. Ferrante, A. Kaliyaperumal, Development of a FRET-based assay for analysis of mAbs internalization and processing by dendritic cells in preclinical immunogenicity risk assessment, AAPS J. (2020), https://doi.org/10.1208/s12248-020-00444-1.
[146] Y.Q. Yang, Y.C. Yang, M.H. Liu, Y.H. Chan, FRET-created traffic light immunoassay based on polymer dots for PSA detection, Anal. Chem. 92 (2020) 1493–1501, https://doi.org/10.1021/acs.analchem.9b04747.
[147] X. Qiu, K.D. Wegner, Y.T. Wu, P.M.P. Van Bergen En Henegouwen, T.L. Jennings, N. Hildebrandt, Nanobodies and antibodies for duplexed EGFR/HER2 immunoassays using terbium-to-quantum dot FRET, Chem. Mater. 28 (2016) 8256–8267, https://doi.org/10.1021/acs.chemmater.6b03198.